INTERNATIONAL JOURNAL OF ADVANCE RESEARCH, IDEAS AND INNOVATIONS IN TECHNOLOGY

ISSN: 2454-132X
Impact factor: 4.295
(Volume 4, Issue 6)
Available online at: www.ijariit.com

Exploring mechanisms for pattern formation through coupled bulk-surface PDES in case of non-linear reactions

Dr. Muflih Alhazmi
alhazmimf1221@gmail.com
Northern Borders University, Arar, Saudi Arabia

ABSTRACT

This work explores mechanisms for pattern formation through coupled bulk-surface partial differential equations of reaction-diffusion type. Reaction-diffusion systems posed both in the bulk and on the surface on stationary volumes are coupled through linear Robin-type boundary conditions. The presented work in this paper studies the case of non-linear reactions in the bulk and surface respectively. For the investigated system is non-dimensionalised and rigorous linear stability analysis is carried out to determine the necessary and sufficient conditions for pattern formation. Appropriate parameter spaces are generated from which model parameters are selected. To exhibit pattern formation, a coupled bulk-surface finite element method is developed and implemented. The numerical algorithm is implemented using an open source software package known as a deal.II and show computational results on spherical and cuboid domains. Also, theoretical predictions of the linear stability analysis are verified and supported by numerical simulations. The results show that non-linear reactions in the bulk and surface generate patterns everywhere.

Keywords— *Bulk-surface, Reaction-diffusion, Finite-Element-Method (FEM), Partial Differential Equations (PDEs)*

1. INTRODUCTION

Most biological and chemical processes that can be explored through reaction and diffusion of chemical species are often modelled by systems of partial differential equations (PDEs) [1-3]. A special class of these are reaction-diffusion equations, which are used to analyse and quantify various biological processes such as the natural evolution of pattern formation on animal coats, developmental embryology, immunology, and ecological dynamics [4-7]. The study of reaction-diffusion systems, in general, has been and continues to be an interesting topic for research in various branches of scientific studies. In order to quantify the evolution of chemical reaction kinetics associated to biological processes, it is a usual approach to employ a system of partial differential equations describing the chemical reactions, which is investigated through mathematical techniques to reveal the long-term behaviour of the evolving kinetics. [8,9]

Alan Turing was one of the first scientists to suggest in 1952 the use of a system of reaction-diffusion equations to model how two or more chemical substances evolve when they are simultaneously subject to a specific reaction rate and each one of them diffuses independently of the other. Alan Turing suggested that the theory of biological pattern formation can be mathematically formulated by a system of partial differential equations [10]. The study [11] is a theoretical set-up through coupling reaction-diffusion system to provide insight on the trajectory of a particle during the process of bulk excursion when it unbinds from the surface without a regular occurrence.

Turing's theory suggests that pattern formation occurs when a system experiences diffusion-driven instability, [10,12] which is a concept that is hypothetically responsible for the emergence of spatial variation in the concentration density of a chemical species. Diffusion-driven instability takes place in the evolution of a system when a uniform stable steady state is destabilised by including the effects of the diffusion process in the system. It is a non-trivial property of the diffusion operator that it can be responsible to destabilise a stable steady state of a system of partial differential equations, because a diffusion operator by itself has the property to homogenise small spatial perturbations, therefore, intuitively if diffusion is added to a system of reaction kinetics that is stable in the absence of diffusion, then small perturbations near a uniform steady state are expected to ensure that the evolution of the reaction-kinetics converges to the uniform steady state.

Researchers in applied mathematics and computational science also explore bulk-surface reaction-diffusion systems (BSRDSs), which are employed in special kinds of models for biological processes, where species react and diffuse in the bulk of a domain and these are coupled with other species that react and diffuse on the surface of the domain. Bulk-surface reaction-diffusion systems are

employed as a framework to model the chemical interaction of bulk-surface problems arising in cell biology. [13] In particular, the framework proposed by [13] aims to provide improved computational and algorithmic efficiency, which is mainly achieved, through employing the usual diffusion on local tangential planes as an approximation of Laplace-Beltrami operator. The framework proposed by [13] is applied to a realistic cell-like geometry, which produces results that are in agreement with quantitative experimental analysis on fluorescence-loss in photo-bleaching. Another example of a computational approach to solving coupled systems of BSRDEs is the work presented in, [14] where they proposed a computational approach to bulk-surface reaction-diffusion systems on time-dependent domains.

In general, there are two main aspects to the study of bulk-surface reaction-diffusion equations. The first approach is to solve systems of bulk-surface numerically. Finite element method is the usual choice of the numerical method in the literature, for example, there is a detailed study in, [15] suggesting some results on the numerical analysis, existence and convergence of finite element approximation when bulk-surface reaction-diffusion equations (BSRDEs) are posed with Robin-type boundary conditions. A priori error bounds on the finite element approximate numerical solution are also both derived in certain norms and verified numerically. The work in [15] is concentrated mainly on the numerical analysis side of the particular scheme they present, which lacks to provide any insight on the stability analysis of the proposed system. Though it is a reasonable decision to exclude stability analysis due to consistency and relevance of contents, however with improvements in computational efficiency of BSRDEs, it is crucial that attention is given to stability analysis of such systems.

Bulk-surface systems with a single PDE posed in the bulk and coupled with another PDE on the surface also play a vital role in understanding the interaction of receptor-ligand in the process of a signaling cascade [16]. In [16] the existence of solutions is proven with some computational results associated with the theoretical problem, again lacking to provide insight into the stability behaviour of the dynamics modelled by the coupled system. Even though the results achieved in are mathematically sound from numerical analysis and computational viewpoint, it would provide a complementary back-up to the work if it is equipped with detailed results of stability analysis.

Stability and bifurcation analysis are two other usual analytical approaches to understanding the dynamical properties of the reaction-diffusion system near a uniform steady state [17-21]. It is evident from the literature on the subject of stability analysis that a very limited amount of work is done on stability analysis in a coupled bulk-surface set-up. This is mainly due to the extensive complexity associated with deriving the relevant conditions for diffusion-driven instability when equations from the bulk are coupled with equations on the surface. One of the first detailed studies on stability analysis of BSRDEs is conducted in, [20] where it is analytically proven that a certain suitable parameter range exists for equations in the bulk that can induce spatial pattern on the surface.

Coupled systems of bulk-surface reaction-diffusion equations (BSRDEs) are one of the several generalisations of reaction-diffusion theory to explore numerous applications in mathematical biology. Processes that involve bulk-surface reaction and/or diffusion are found in various research disciplines such as experimental research in organic chemistry, where a bulk-surface photografting process is used as an efficient tool to create thick grafted layers of hydrophobic polymers in a very short span of time. [22,23]

Bulk-surface reaction kinetics are also used to investigate the behaviour of chemical reactions in the interior of a cell, and to explore how a set of specific reaction kinetics in the interior of a cell evolve to influence the surface of the cell. [25] We also find bulk-surface reaction-diffusion equations that model a particular aspect of cellular functions with relevance to chemical signalling. In [25] a detailed mathematical model is developed for this particular investigation, to explore the dynamics of pattern formation in the consequences of bulk-surface coupling reaction kinetics. Moreover, bulk-surface reaction-diffusion equations help to reveal the mechanism of symmetry breaking which is one of the essential steps before the emergence of polarisation of biological cells or buds in yeast cells, the direction of cell motility. [25]

The bulk-surface reaction-diffusion system is also used to model how surface active agents (surfactants) evolve on the surface of a system, in which the chemical concentration is coupled through a given reaction with the substance in the bulk [26]. BSRDSs also arise in mathematical models for the dynamics of lipid raft formation on biological membranes [27], where the formation of the layer on a biological membrane is modelled as the consequence of coupling conditions with species that react and diffuse in the bulk. A further example of a biological application employing bulk-surface reaction-diffusion systems is presented in [28], where they model the mediation of cellular metabolism and signalling in part by trans-membrane receptors that undergo the process of diffusion in the cell membrane. From the variety of applications that employ BSRDSs, one realises that a robust study of such systems can provide solutions to a great number of important questions in mathematical biology. This, in turn, requires an in-depth and rigorous study of BSRDSs in an attempt to achieve extensive insight into the evolving properties of these models. Most of the published work presented in the current section on the study of BSRDSs either investigate an over-simplified case scenario with the aim of mathematical tractability or a complex model with limitations on the robustness of analytical and numerical findings.

In this paper, the presented study is motivated to explore BSRDSs with a realistic degree of complexity through a four-component reaction-diffusion system, two of which are posed on the surface and the other two are posed the bulk. The equations in the bulk and on the surface also satisfy coupling conditions through the evolution dynamics on the surface is influenced by the reaction-diffusion process inside the bulk. It can prove of great importance to obtain insight on the pattern formation properties of such systems. The tools to achieve this in the current thesis are the combined application of linear stability theory, mode isolation and the finite element method.

The remaining part of the paper is organised as follows. Section 2 a study is conducted through the application of rigorous linear stability theory which is applied to analytically explore and predict the pattern formation properties associated with the adopted

bulk-surface reaction-diffusion system. This is done by investigating the necessary conditions for diffusion-driven instability for the system. Section 3 presents deriving a set of sufficient conditions for diffusion-driven instability, which complements the necessary conditions of the previous section in order to insure that spatial pattern is obtained. In Section 4 the theoretical formulation for the finite element method is presented for the investigated system. Section 5 contains the numerical simulations obtained using Deal.II library to verify the analytical predictions associated with the pattern formation properties for the three systems. Finally, section 6 concludes the presented work in this paper.

2. ANALYSIS OF COUPLED SYSTEM OF BULK-SURFACE REACTION-DIFFUSION EQUATIONS (BSRDES)

In this section, we formulate and present the coupled systems of bulk-surface reaction-diffusion equations on stationary volumes, in which two of the equations are posed in the bulk and coupled with two other equations that are posed on the surface bounding the corresponding stationary volume. Reaction-diffusion systems posed both in the bulk and on the surface are coupled through linear Robin-type boundary conditions.

For the investigated system, we analyse non-linear reaction kinetics both in the bulk and on the surface. The details of the scaling process that makes the system studied in this paper dimensionless are presented. Also, linear stability analysis is carried out both in the absence and presence of diffusion, the necessary and sufficient conditions for the steady state to be stable are derived in the absence of diffusion. In the presence of diffusion, the necessary conditions for diffusion-driven instability are derived. The theoretical results for this system show that the bulk dynamics and the surface dynamics drive pattern formation.

Let $\Omega \subset \mathbb{R}^3$ be a stationary domain with boundary that is a compact hyper surface denoted by $\Gamma \subset \mathbb{R}^2$. Let $u: \Omega \times (0,T] \to \mathbb{R}$ and $v: \Omega \times (0,T] \to \mathbb{R}$ denote the concentration of two chemical species which react and diffuse in Ω. Let $r: \Gamma \times (0,T] \to \mathbb{R}$ and $s: \Gamma \times (0,T] \to \mathbb{R}$ denote two chemical species residing on the surface.

When the species from the bulk and surface are coupled only through the reaction kinetics and there is no cross-diffusion, it means that all four species diffuse independently of each other, which can be written in dimensional form with independent diffusion rates as follow:

$$\begin{cases} \begin{cases} u_t &= D_u \Delta u + f(u,v), \\ v_t &= D_v \Delta v + g(u,v), \end{cases} & \text{in } \Omega \times (0,T] \\ \begin{cases} r_t &= D_r \Delta_\Gamma r + f(r,s) - h_1(u,v,r,s), \\ s_t &= D_s \Delta_\Gamma s + g(r,s) - h_2(u,v,r,s), \end{cases} & \text{on } \Gamma \times (0,T] \end{cases} \tag{1}$$

With coupling boundary conditions

$$\begin{cases} \dfrac{\partial u}{\partial \boldsymbol{\nu}} = h_1(u,v,r,s), \\ d_\Omega \dfrac{\partial v}{\partial \boldsymbol{\nu}} = h_2(u,v,r,s), \end{cases} \quad \text{on } \Gamma \times (0,T]. \tag{2}$$

Where, Ω is a three-dimensional fixed domain bounded by a compact surface denoted by Γ, which means that it is a boundary-free connected and closed surface. The strictly positive constants $D_u > 0$, $D_v > 0$, $D_r > 0$ and $D_s > 0$ are the independent diffusion rates corresponding to the variables indicated in the respective subscripts of each D.

We assume $f(.,.)$ and $g(.,.)$ to be non-linear functions. The coupling conditions of the system are represented by h_1 and h_2 which are functions of u, v, r and s. h_1 and h_2 denote reactions of substances througth boundary interface, therefore they depend on all four species namely u, v, r and s.

We explicitly define $h_1(u,v,r,s)$ and $h_2(u,v,r,s)$ [20] to be:

$$h_1(u,v,r,s) = \alpha_1 r - \beta_1 u - \kappa_1 v \tag{3}$$

$$h_2(u,v,r,s) = \alpha_2 s - \beta_2 u - \kappa_2 v. \tag{4}$$

The constants $\alpha_1, \alpha_2, \beta_1, \beta_2, \kappa_1$ and κ_2 are positive parameters of system (1). We also assume that from all the species we initially have some positive quantity present, which we denote by u^0, v^0, r^0 and s^0, which provides the initial conditions for system (1) written as:

$$u(\mathbf{x},0) = u^0(\mathbf{x}), \quad v(\mathbf{x},0) = v^0(\mathbf{x}), \quad r(\mathbf{x},0) = r^0(\mathbf{x}), \quad \text{and} \quad s(\mathbf{x},0) = s^0(\mathbf{x}).$$

In this system, we focus on the widely known *activator-depleted* model also known as the Brusselator Model [29-33]. In the Brusselator Model, the reaction kinetics are non-linear, given by

$$f(u,v) = k_1 - k_2 u + k_3 u^2 v, \quad \text{and} \quad g(u,v) = k_4 - k_3 u^2 v, \tag{5}$$

With positive parameters k_1, k_2, k_3 and k_4.

2.1 Non-Dimensionalisation

The system of equations is non-dimensionalised using a specific scale, in space or time, for observing the prospective solution within the specified scale range. In the new system after non-dimensionalisation, the variables and parameters are all unitless and the parameters will be fewer than in system (1). The non-dimensional variables are introduced with a hat and these are written as $\hat{u}$, $\hat{v}$, $\hat{r}$ and $\hat{s}$ with the corresponding scaling factors u^*, v^*, r^* and s^* respectively. The process of non-dimensionalisation is only represented for the bulk-equations in three spatial diemnsions, and the process is identical to non-dimensionalise the surface equations where a two-dimensional surface is embedded in three dimensional space. We choose L to denote the scaling factor for length (L_b for the bulk and L_s for the surface) and t^* to denote the scaling factor for time (t_b^* for the bulk and t_s^* for the surface), The dimensional and the non-dimensional variables [34,35], are related through

$$u = u^*\hat{u}, \qquad v = v^*\hat{v}, \qquad r = r^*\hat{r}, \qquad s = s^*\hat{s},$$

Where for the bulk we use the scaling given by:

$$x = L_b\hat{x}, \qquad y = L_b\hat{y}, \qquad z = L_b\hat{z}, \qquad t = t_b^*\tau$$

and for the surface equations, we use:

$$x = L_s\hat{x}, \qquad y = L_s\hat{y}, \qquad z = L_s\hat{z}, \qquad t = t_s^*\tau.$$

We substitute for each dimensional variable its corresponding product of a non-dimensional variable and the scaling factor leading to:

$$\frac{u^*}{t_b^*}\frac{\partial\hat{u}}{\partial\tau} = D_u\frac{u^*}{L_b^2}\Delta\hat{u} + k_1 - k_2u^*\hat{u} + k_3u^{*2}v^*\hat{u}^2\hat{v}, \tag{6}$$

$$\frac{v^*}{t_b^*}\frac{\partial\hat{v}}{\partial\tau} = D_v\frac{v^*}{L_b^2}\Delta\hat{v} + k_4 - k_3u^{*2}v^*\hat{u}^2\hat{v}, \qquad \text{in } \hat{\Omega}\times(0,\hat{T}] \tag{7}$$

$$\frac{r^*}{t_s^*}\frac{\partial\hat{r}}{\partial\tau} = D_r\frac{r^*}{L_s^2}\Delta_{\hat{\Gamma}}\hat{r} + k_1 - k_2r^*\hat{r} + k_3r^{*2}s^*\hat{r}^2\hat{s} - \alpha_1r^*\hat{r} + \beta_1u^*\hat{u} + \kappa_1v^*\hat{v}, \tag{8}$$

$$\frac{s^*}{t_s^*}\frac{\partial\hat{s}}{\partial\tau} = D_s\frac{s^*}{L_s^2}\Delta_{\hat{\Gamma}}\hat{s} + k_4 - k_3r^{*2}s^*\hat{r}^2\hat{s} - \alpha_2s^*\hat{s} + \beta_2u^*\hat{u} + \kappa_2v^*\hat{v}, \quad \text{on } \hat{\Gamma}\times(0,\hat{T}] \tag{9}$$

Where $\hat{\Omega}$ and $\hat{\Gamma}$ respectively denote unit cube and its six sided surface. The scaling $\hat{T}$ denotes the final time for the non-dimensional system.

Multiplying (6), (7), (8) and (9) by $\frac{t_b^*}{u^*}$, $\frac{t_b^*}{v^*}$, $\frac{t_s^*}{r^*}$ and $\frac{t_s^*}{s^*}$ respectively, provided that u^*, v^*, r^* and s^* are non-zero. We may choose to define $t_b^* = \frac{L_b^2}{D_u}$ and $t_s^* = \frac{L_s^2}{D_r}$ and factoring out some parameters will result in writing the system as

$$\begin{cases} \dfrac{\partial\hat{u}}{\partial\tau} = \Delta\hat{u} + \dfrac{L_b^2k_2}{D_u}\left[\dfrac{k_1}{k_2u^*} - \hat{u} + \dfrac{k_3}{k_2}u^{*2}v^*\hat{u}^2\hat{v}\right], \\ \dfrac{\partial\hat{v}}{\partial\tau} = d_\Omega\Delta\hat{v} + \dfrac{L_b^2k_2}{D_u}\left[\dfrac{k_4}{k_2v^*} - \dfrac{k_3}{k_2}u^{*2}\hat{u}^2\hat{v}\right], \end{cases} \quad \text{in } \hat{\Omega}\times(0,\hat{T}] \\ \begin{cases} \dfrac{\partial\hat{r}}{\partial\tau} = \Delta_{\hat{\Gamma}}\hat{r} + \dfrac{L_s^2k_2}{D_r}\left[\dfrac{k_1}{r^*k_2} - \hat{r} + \dfrac{k_3}{k_2}r^{*2}s^*\hat{r}^2\hat{s} - \dfrac{\alpha_1}{k_2}\hat{r} + \dfrac{u^*}{r^*k_2}\beta_1\hat{u} + \dfrac{v^*}{r^*k_2}\kappa_1\hat{v}\right], \\ \dfrac{\partial\hat{s}}{\partial\tau} = d_\Gamma\Delta_{\hat{\Gamma}}\hat{s} + \dfrac{L_s^2k_2}{D_r}\left[\dfrac{k_4}{s^*k_2} - \dfrac{k_3}{k_2}r^{*2}\hat{r}^2\hat{s} - \dfrac{\alpha_2}{k_2}\hat{s} + \dfrac{u^*}{s^*k_2}\beta_2\hat{u} + \dfrac{v^*}{s^*k_2}\kappa_2\hat{v}\right], \end{cases} \text{on } \hat{\Gamma}\times(0,\hat{T}] \tag{10}$$

Where $d_\Omega = \frac{D_v}{D_u}$ and $d_\Gamma = \frac{D_s}{D_r}$ express the non-dimensional positive ratios of diffusion parameters. Requiring the terms $\frac{k_3}{k_2}u^{*2} = 1$ and $\frac{k_3}{k_2}r^{*2} = 1$ to be non-dimensional respectively imply defining $u^* = \sqrt{\frac{k_2}{k_3}}$ and $r^* = \sqrt{\frac{k_2}{k_3}}$. The scaling factors v^* and s^* through a similar process may be derived as

$$\frac{k_3}{k_2}\sqrt{\frac{k_2}{k_3}}v^* = 1 \Rightarrow v^* = \sqrt{\frac{k_2}{k_3}} \quad \text{and} \quad \frac{k_3}{k_2}\sqrt{\frac{k_2}{k_3}}s^* = 1 \Rightarrow s^* = \sqrt{\frac{k_2}{k_3}}. \tag{11}$$

Substituting (11) in system (10) results in

$$\begin{cases} \dfrac{\partial\hat{u}}{\partial\tau} = \Delta\hat{u} + \gamma_\Omega[a_2 - \hat{u} + \hat{u}^2\hat{v}], \\ \dfrac{\partial\hat{v}}{\partial\tau} = d_\Omega\Delta\hat{v} + \gamma_\Omega[b_2 - \hat{u}^2\hat{v}], \end{cases} \quad \text{in } \hat{\Omega}\times(0,\hat{T}] \\ \begin{cases} \dfrac{\partial\hat{r}}{\partial\tau} = \Delta_{\hat{\Gamma}}\hat{r} + \gamma_\Gamma[a_2 - \hat{r} + \hat{r}^2\hat{s} - \rho_3\hat{r} + \mu\hat{u} + \delta_2\hat{v}], \\ \dfrac{\partial\hat{s}}{\partial\tau} = d_\Gamma\Delta_{\hat{\Gamma}}\hat{s} + \gamma_\Gamma[b_2 - \hat{r}^2\hat{s} - \rho_4\hat{s} + \mu_1\hat{u} + \delta_3\hat{v}], \end{cases} \quad \text{on } \hat{\Gamma}\times(0,\hat{T}] \tag{12}$$

where the new dimensionless parameters $\gamma_\Omega = \frac{L_b^2k_2}{D_u}$, $\gamma_\Gamma = \frac{L_s^2k_2}{D_r}$, $a_2 = \frac{k_1\sqrt{\frac{k_3}{k_2}}}{k_2}$, $b_2 = \frac{k_4\sqrt{\frac{k_3}{k_2}}}{k_2}$, $\rho_3 = \frac{\alpha_1}{k_2}$, $\rho_4 = \frac{\alpha_2}{k_2}$, $\mu = \frac{\beta_1}{k_2}$, $\mu_1 = \frac{\beta_2}{k_2}$, $\delta_2 = \frac{\kappa_1}{k_2}$ and $\delta_3 = \frac{\kappa_2}{k_2}$ are defined as a consequence of the scaling choice used for u^*, v^*, r^* and s^*.

The boundary and initial conditions are non-dimensionalised through the same choice of scaling factors for all variables. For notational convenience, we drop all the hats from the non-dimensional variables to obtain the full system of BSRDEs given by (1) in its non-dimensional form as

$$\begin{cases} \dfrac{\partial u}{\partial t} = \Delta u + \gamma_\Omega[a_2 - u + u^2v], \\ \dfrac{\partial v}{\partial t} = d_\Omega\Delta v + \gamma_\Omega[b_2 - u^2v], \end{cases} \quad \text{in } \Omega\times(0,T] \\ \begin{cases} \dfrac{\partial r}{\partial t} = \Delta_\Gamma r + \gamma_\Gamma[a_2 - r + r^2s - \rho_3r + \mu u + \delta_2v], \\ \dfrac{\partial s}{\partial t} = d_\Gamma\Delta_\Gamma s + \gamma_\Gamma[b_2 - r^2s - \rho_4s + \mu_1u + \delta_3v], \end{cases} \quad \text{on } \Gamma\times(0,T] \tag{13}$$

With linear boundary conditions

$$\begin{cases} \nabla u \cdot \boldsymbol{\nu} = \gamma_\Gamma[\rho_3 r - \mu u - \delta_2 v], \\ d_\Omega \nabla v \cdot \boldsymbol{\nu} = \gamma_\Gamma[\rho_4 s - \mu_1 u - \delta_3 v]. \end{cases} \quad \text{on } \Gamma \times (0,T], \tag{14}$$

The non-dimensional initial conditions for all equations are given by

$$u(\mathbf{x},0) = u^0(\mathbf{x}), \;\; v(\mathbf{x},0) = v^0(\mathbf{x}), \;\; r(\mathbf{x},0) = r^0(\mathbf{x}) \;\text{ and }\; s(\mathbf{x},0) = s^0(\mathbf{x}). \tag{15}$$

The parameter γ_Ω is known as the reaction scaling parameter in the bulk and γ_Γ is the reaction scaling parameter on the surface and both are non-dimensional.

2.2 Linear stability analysis in the absence of diffusion

DEFINITION 2.1 *(Uniform steady state):* [10,12] *A point* (u_0, v_0, r_0, s_0) *is a uniform steady state of the coupled system of bulk-surface reaction-diffusion equations* (13) *if it solves the non-linear algebraic system given by* $f_i(u_0, v_0, r_0, s_0) = 0$, *for all* $i =$ 1,2,3,4 *and satisfies the boundary conditions given by* (14)

We derive the uniform steady state by solving the algebraic system

$$f_1(u,v,r,s) = \gamma_\Omega(a_2 - u + u^2 v) = 0, \tag{16}$$
$$f_2(u,v,r,s) = \gamma_\Omega(b_2 - u^2 v) = 0, \tag{17}$$
$$f_3(u,v,r,s) = \gamma_\Gamma(a_2 - r + r^2 s - \rho_3 r + \mu u + \delta_2 v) = 0, \tag{18}$$
$$f_4(u,v,r,s) = \gamma_\Gamma(b_2 - r^2 s - \rho_4 s + \mu_1 u + \delta_3 v) = 0, \tag{19}$$

Such that the boundary conditions given by (14) are also satisfied:

$$\gamma_\Gamma[\rho_3 r - \mu u - \delta_2 v] = 0, \tag{20}$$
$$\gamma_\Gamma[\rho_4 s - \mu_1 u - \delta_3 v] = 0. \tag{21}$$

We add (16) and (17) to obtain

$$a_2 - u_0 - u_0^2 v_0 + b_2 - u_0^2 v_0 = 0 \;\Rightarrow u_0 = a_2 + b_2. \tag{22}$$

Upon substituting u_0 into (17), we find

$$v_0 = \frac{b_2}{(a_2 + b_2)^2}.$$

Through similar straightforward algebraic manipulation, we also find the steady state expressions for r_0 and s_0 in the form

$$r_0 = a_2 + b_2, \quad \text{and} \quad s_0 = \frac{b_2}{(a_2 + b_2)^2}. \tag{23}$$

Therefore, the uniform steady state solution satisfying system (13) is of the form

$$(u_0, v_0, r_0, s_0) = (a_2 + b_2, \frac{b_2}{(a_2 + b_2)^2}, a_2 + b_2, \frac{b_2}{(a_2 + b_2)^2}). \tag{24}$$

Substituting the uniform steady state (24) in (18) and (19) leads to state condition on the parameters. The condition on the parameters is derived by direct substitution of (24) and algebraic manipulations through the following steps result in

$$-\rho_3(a_2 + b_2) + \mu(a_2 + b_2) + \delta_2 \frac{b_2}{(a_2 + b_2)^2} = 0, \tag{25}$$
$$\Rightarrow (a_2 + b_2)^3 = -\frac{b_2 \delta_2}{\mu - \rho_3}.$$

$$-\rho_4 \frac{b_2}{(a_2 + b_2)^2} + \mu_1(a_2 + b_2) + \delta_3 \frac{b_2}{(a_2 + b_2)^2} = 0, \tag{26}$$
$$\Rightarrow (a_2 + b_2)^3 = -\frac{b_2(\delta_3 - \rho_4)}{\mu_1}.$$

Combining (25) and (26) we obtain the required condition on the parameters in the form

$$\frac{b_2 \delta_2}{\mu - \rho_3} = \frac{b_2(\delta_3 - \rho_4)}{\mu_1},$$
$$(\mu - \rho_3)(\delta_3 - \rho_4) = \delta_2 \mu_1. \tag{27}$$

Therefore, in order for (24) to be a steady state of the system (13), a condition on the parameters is required to hold, which is

$$(\mu - \rho_3)(\delta_3 - \rho_4) - \delta_2 \mu_1 = 0. \tag{28}$$

These findings are summarized in the following theorem.

THEOREM 2.1 *(Existence and uniqueness of the uniform steady state) [20] The coupled system of BSRDEs* (13) *with conditions* (14) *admits a unique non-zero steady state given by*

$$(u_0, v_0, r_0, s_0) = (a_2 + b_2, \frac{b_2}{(a_2 + b_2)^2}, a_2 + b_2, \frac{b_2}{(a_2 + b_2)^2}), \tag{29}$$

Provided the following compatibility condition on the coefficients of the coupling terms is satisfied

$$(\mu - \rho_3)(\delta_3 - \rho_4) - \delta_2 \mu_1 = 0. \tag{30}$$

Finally, we set out the summary of the necessary and sufficient conditions for $\mathrm{Re}(\lambda) < 0$ in Theorem 2.2.

THEOREM 2.2 *(Necessary and sufficient conditions for* $\mathrm{Re}(\lambda) < 0$ *)* [10,12] *The necessary and sufficient conditions such that the zeros of the polynomial* $p_4(\lambda)$ *have* $\mathrm{Re}(\lambda) < 0$ *are given by the following condition:*

$$f_{1u} + f_{2v} < 0, \tag{31}$$
$$f_{1u}f_{2v} - f_{1v}f_{2u} > 0, \tag{32}$$
$$f_{3r} + f_{4s} < 0, \tag{33}$$
$$f_{3r}f_{4s} - f_{3s}f_{4r} > 0. \tag{34}$$

2.3 Linear stability analysis in the presence of diffusion

We start by analysing the system by taking the diffusion terms into account and performing the linear stability analysis. We introduce a small perturbation in the neighbourhood of the steady state namely (u_0, v_0, r_0, s_0). We introduce the small perturbations up to the linear term in the form of

$$u(\mathbf{x}, t) = u_0 + \varepsilon w_1(\mathbf{x}, t),$$
$$v(\mathbf{x}, t) = v_0 + \varepsilon w_2(\mathbf{x}, t),$$
$$r(y, t) = r_0 + \varepsilon w_3(y, t),$$
$$s(y, t) = s_0 + \varepsilon w_4(y, t),$$
$$\text{where} \quad 0 < \varepsilon << 1.$$

If we substitute these small perturbations into the system we obtain

$$\frac{\partial u(\mathbf{x}, t)}{\partial t} = \frac{\partial (u_0 + \varepsilon w_1(\mathbf{x}, t))}{\partial t} = \varepsilon \frac{\partial w_1(\mathbf{x}, t)}{\partial t},$$
$$\frac{\partial v(\mathbf{x}, t)}{\partial t} = \frac{\partial (v_0 + \varepsilon w_2(\mathbf{x}, t))}{\partial t} = \varepsilon \frac{\partial w_2(\mathbf{x}, t)}{\partial t},$$
$$\frac{\partial r(y, t)}{\partial t} = \frac{\partial (r_0 + \varepsilon w_3(y, t))}{\partial t} = \varepsilon \frac{\partial w_3(y, t)}{\partial t},$$
$$\frac{\partial s(y, t)}{\partial t} = \frac{\partial (s_0 + \varepsilon w_4(y, t))}{\partial t} = \varepsilon \frac{\partial w_4(y, t)}{\partial t}$$

and also

$$\begin{aligned} \Delta u(\mathbf{x}, t) &= \Delta(u_0 + \varepsilon w_1(\mathbf{x}, t)) = \varepsilon \Delta w_1(\mathbf{x}, t), \\ d_\Omega \Delta v(\mathbf{x}, t) &= d_\Omega \Delta(v_0 + \varepsilon w_2(\mathbf{x}, t)) = d_\Omega \varepsilon \Delta w_2(\mathbf{x}, t), \\ \Delta_\Gamma r(y, t) &= \Delta_\Gamma(r_0 + \varepsilon w_3(y, t)) = \varepsilon \Delta_\Gamma w_3(y, t), \\ d_\Gamma \Delta_\Gamma s(y, t) &= d_\Gamma \Delta_\Gamma(s_0 + \varepsilon w_4(y, t)) = d_\Gamma \varepsilon \Delta_\Gamma w_4(y, t). \end{aligned}$$

Similarly, we substitute such perturbations in the reaction terms. Since we know that at the steady state $f(u_0, v_0, r_0, s_0)$, $g(u_0, v_0, r_0, s_0)$, $h_1(u_0, v_0, r_0, s_0)$ and $h_2(u_0, v_0, r_0, s_0)$ are all equal zero, therefore we aim to collect terms in such a way to determine the relative expressions for the steady state in each equation. Furthermore, we aim to perform linear stability aa nalysis. Performing the algebra and cancelling the expressions for steady state and ignoring higher order terms will transform the equations into linearised system the a of equations.

For the remaining of this work, the analysis is restricted to circular and spherical domains, where the cartesian coordinates are transformed to polar coordinates. The coordinate transformation is done mainly for the convenience of applying the separation variables. A close form solution can be written in the form

$$\begin{aligned} w_1(\mathbf{x}, t) &= \psi_{k_{l,m}}(\mathbf{x}) u_{l,m}(t), \\ w_2(\mathbf{x}, t) &= \psi_{k_{l,m}}(\mathbf{x}) v_{l,m}(t), \\ w_3(y, t) &= \phi(y) r_{l,m}(t), \\ w_4(y, t) &= \phi(y) s_{l,m}(t), \end{aligned}$$

which are substituted in the linearised system of equations, to obtain

$$\psi_{k_{l,m}}(\mathbf{x}) u'_{l,m}(t) = \Delta \psi_{k_{l,m}}(\mathbf{x}) u_{l,m}(t),$$
$$\psi_{k_{l,m}}(\mathbf{x}) v'_{l,m}(t) = \Delta \psi_{k_{l,m}}(\mathbf{x}) v_{l,m}(t),$$
$$\phi(y) r'_{l,m}(t) = \Delta_\Gamma \phi(y) r_{l,m}(t),$$
$$\phi(y) s'_{l,m}(t) = \Delta_\Gamma \phi(y) s_{l,m}(t).$$

For equations on the surface, the relations may be written as

$$\frac{r'_{l,m}(t)}{r_{l,m}(t)} = \frac{\Delta_\Gamma \phi(y)}{\phi(y)} = -l(l+1),$$
$$\frac{s'_{l,m}(t)}{s_{l,m}(t)} = \frac{\Delta_\Gamma \phi(y)}{\phi(y)} = -l(l+1),$$

Whereas for the bulk, the relations take the form

$$\frac{u'_{l,m}(t)}{u_{l,m}(t)} = \frac{\Delta \psi_{k_{l,m}}(\mathbf{x})}{\psi_{k_{l,m}}(\mathbf{x})} = -k^2_{l,m},$$
$$\frac{v'_{l,m}(t)}{v_{l,m}(t)} = \frac{\Delta \psi_{k_{l,m}}(\mathbf{x})}{\psi_{k_{l,m}}(\mathbf{x})} = -k^2_{l,m}.$$

We consider a coordinate transformation in which a vector $\mathbf{x}$ may define every point in the bulk by the variables r (radial distance from the origin) and $\mathbf{y}$ (a point on the surface), with the relationship $\mathbf{x} = r\mathbf{y}$ where $r \in (0,1)$, $\mathbf{y} \in \Gamma$.

Since the eigenvalue of the problem on the surface depends on l itself, therefore we may consider positive integers only, and m can be any integer with the restriction $|m| \leq l$. This is because the eigenvalues of both problems are equal at $r = 1$. Note that if $r = 1$ for the eigenvalue problem in the bulk, then the eigenvalues associated to the usual diffusion operator must coincide with those associated to Laplace-Beltrami operator on the surface, which means the following relation must hold.

$$-k_{l,m}^2 = -l(l+1)$$

Now we summarise the results in the following theorem.

THEOREM 2.3: [10,12] *The necessary conditions for diffusion-driven instability for the coupled system of BSRDEs* (13) *and* (14) *are given by*

$$f_{1u} + f_{2v} < 0, \tag{35}$$
$$f_{1u}f_{2v} - f_{1v}f_{2u} > 0, \tag{36}$$
$$f_{3r} + f_{4s} < 0, \tag{37}$$
$$f_{3r}f_{4s} - f_{3s}f_{4r} > 0, \tag{38}$$

and,

$$d_\Omega f_{1u} + f_{2v} > 0 \quad \text{and} \quad [d_\Omega f_{1u} + f_{2v}]^2 - 4d_\Omega(f_{1u}f_{2v} - f_{1v}f_{2u}) > 0. \tag{39}$$

and/or

$$d_\Gamma f_{3r} + f_{4s} > 0 \quad \text{and} \quad [d_\Gamma f_{3r} + f_{4s}]^2 - 4d_\Gamma(f_{3r}f_{4s} - f_{3s}f_{4r}) > 0. \tag{40}$$

3. MODE ISOLATION AND PARAMETER SPACE GENERATION

In this section, we proceed with the process of deriving sufficient conditions for diffusion-driven instability that complement the necessary conditions found in section 2 to ensure the emergence of spatial patterns. As the standard requirement of this process, we start by extracting excitable wavenumber through the analysis of critical diffusion ratio. Eigenvalues and eigenfunctions of the Laplace operator are briefly discussed on the surface. The results for mode isolation for the excitable wavenumber are employed to computationally find Turing parameter spaces on the real positive parameter plane. We also present the process of coordinate transformation from cartesian to spherical of the usual Laplace operator. Finally, we analyse and compare the shift and dependence of Turing spaces for equations in the bulk with those Turing spaces that are derived for equations on the surface.

3.1 Critical diffusion ratio and excitable wavenumber

For the bulk, the conditions (35), (36) and (39) are necessary but not sufficient for the emergence of an inhomogeneous spatial structure. The sufficient condition requires the existence of some finite wavenumber $k^2 \in (k_-^2, k_+^2)$, where $k_\pm^2$ are the roots of the equation $H_2(k^2) = 0$. Also, for the surface the conditions (37), (38) and (41) are necessary but not sufficient for diffusion-driven instability and the sufficient condition requires the existence of some finite wavenumber $l(l+1) \in (l(l+1)_-, l(l+1)_+)$ where $l(l+1)_\pm$ are the roots of the equation $H_1(l(l+1)) = 0$.

When the minimum $H_2(k^2) = 0$, we require that

$$f_{1u}f_{2v} - f_{1v}f_{2u} = \frac{(d_c f_{1u} + f_{2v})^2}{4d_c}. \tag{41}$$

For fixed parameters on the kinetics in the bulk, the critical diffusion d_c is obtained using the following form

$$d_c^2 f_{1u}^2 - (2f_{1u}f_{2v} - 4f_{1v}f_{2u})d_c + f_{2v}^2 = 0. \tag{42}$$

Corresponding to the critical diffusion coefficient d_c, there exists a critical wave number k_c^2, which is the root of the polynomial

$$H_2(k_{l,m}^2) = {k_{l,m}}^4 d_\Omega - {k_{l,m}}^2 \gamma_\Omega[d_\Omega f_{1u} + f_{2v}] + (f_{1u}f_{2v} - f_{1v}f_{2u})\gamma_\Omega^2 = 0. \tag{43}$$

The expression for k_c^2 that obtained by

$$k_c^2 = \pm\gamma_\Omega\sqrt{\frac{(f_{1u}f_{2v} - f_{1v}f_{2u})}{d_c}}. \tag{44}$$

This is the critical wavenumber, the sufficient condition for Turing instability with the necessary conditions (35), (36) and (39) satisfied, which leads the system to evolve into a spatial pattern. Similarly, the critical diffusion coefficient d_c on the surface can be obtained from the following equation:

$$d_c^2 f_{3r}^2 - (2f_{3r}f_{4s} - 4f_{3s}f_{4r})d_c + f_{4s}^2 = 0. \tag{45}$$

The critical wavenumber on the surface is given by

$$l(l+1)_c = \pm\gamma_\Gamma\sqrt{\frac{(f_{3r}f_{4s} - f_{3s}f_{4r})}{d_c}}, \tag{46}$$

Which provides sufficient condition for diffusion-driven instability on the surface.

For fixed kinetics parameter values, $a_2 = 0.1$, $b_2 = 0.9$, we use the first derivatives of f_1, f_2, f_3 and f_4 and the values $u_0 = a_2 + b_2 = 0.1 + 0.9 = 1$, $v_0 = \frac{b_2}{(a_2+b_2)^2} = 0.9$,.

Substituting these values into (42), one obtains

$$d_c^2(0.64) - (5.6)d_c + 1 = 0,$$

For which the two roots are given by

$$d_c = 8.56762745781 > 1, \quad (47)$$

$$d_c = 0.18237254218 < 1. \quad (48)$$

Since the diffusion coefficient must be greater than 1, then we only take the critical diffusion coefficient ratio as $d_c = 8.56762745781$.

Figure 1(a) shows the plot of $H_2(k^2)$ as a function of k^2. All three possibilities for diffusion coefficient d with respect to the critical diffusion d_c are plotted.

To verify that $d < d_c$ does not allow Turing pattern to evolve, the necessary conditions are tested on the parameter space (a_2, b_2) where a_2 and b_2 are the positive constants of the Schnakenberg reaction kinetics. It is found that when $d < d_c$, there is no region in the parameter space that would become unstable due to diffusion in the system. This is shown in figure 2(a). Similarly when $d > d_c$, then we see that the unstable region is formed in the parameter space (yellow region in figure 2(b)), which corresponds to the parameter values that would result in the system to evolve into a Turing pattern.

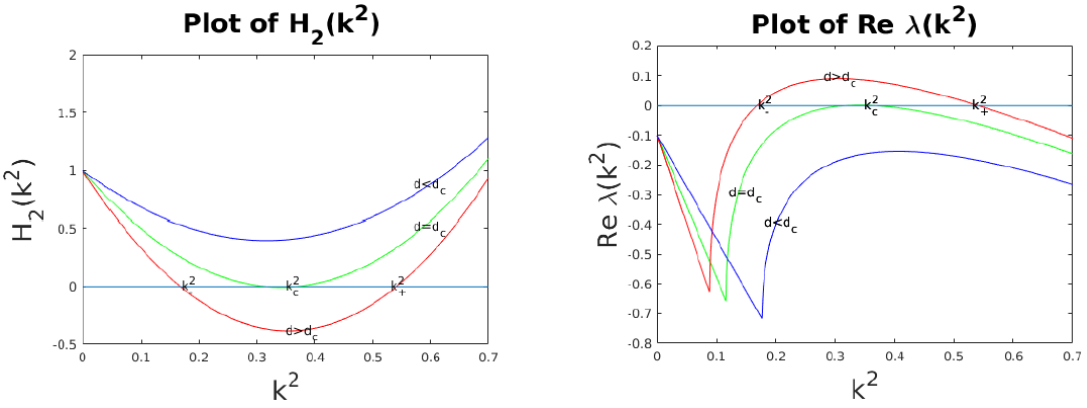

(a) **(b)**

Fig. 1: Plot of $H_2(k^2)$ is shown in (a). When d > dc, then $H_2(k^2) < 0$ for a finite range of $k^2 > 0$: Plot of the largest of the eigenvalue $\lambda(k^2)$ as a function of k^2 is shown in (b). When d > dc, there is a range of wavenumbers $k_-^2 < k^2 < k_+^2$ which are linearly unstable

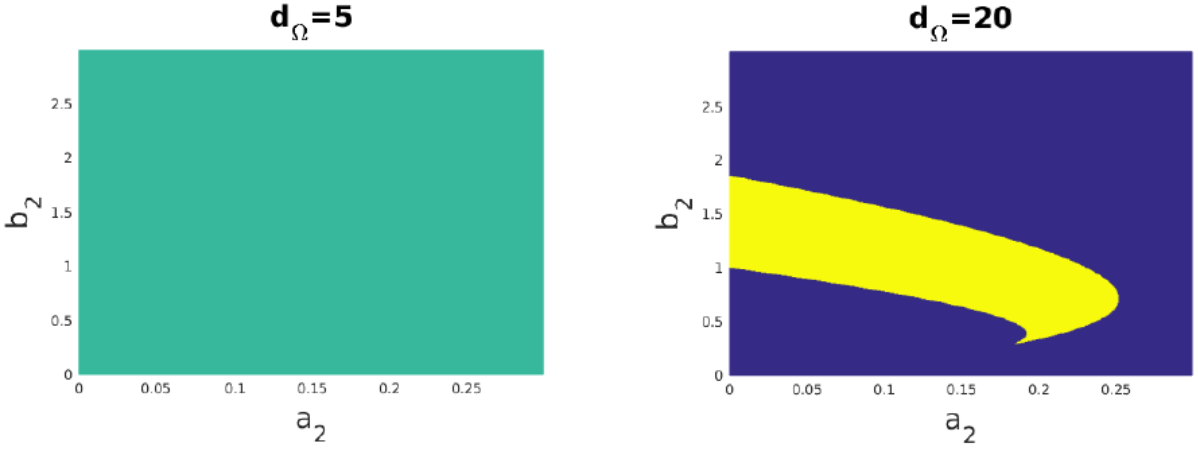

(a) **(b)**

Fig. 2: When d < dc, then there is no region in parameter space that corresponds to Turing instability, which is shown in (a). When d > dc, then the diffusion-driven instability region in parameter space exists that corresponds to Turing instability and is shown in (b).

3.2 Mode isolation in the bulk

With the help of linear stability analysis, certain modes can be isolated to help find the admissible set of parameter values d_Ω and γ_Ω for diffusion-driven instability. The necessary conditions for diffusion-driven instability found in section 2 are

$$f_{1u} + f_{2v} < 0, \quad (49)$$

$$f_{1u}f_{2v} - f_{1v}f_{2u} > 0, \quad (50)$$

$$d_\Omega f_{1u} + f_{2v} > 0 \quad \text{and} \quad [d_\Omega f_{1u} + f_{2v}]^2 - 4d_\Omega(f_{1u}f_{2v} - f_{1v}f_{2u}) > 0. \quad (51)$$

One of the sufficient conditions, however, for diffusion-driven instability is that the eigenvalues of the Laplace operator should fall in the real interval between the small and the large eigenvalues of the system. It means that

$$\gamma L = k_-^2 < k^2 < k_+^2 = \gamma R \quad (52)$$

Must hold with L and R expressed by:

$$L = \frac{(d_\Omega f_{1u} + f_{2v}) - \sqrt{(d_\Omega f_{1u} + f_{2v})^2 - 4d_\Omega(f_{1u}f_{2v} - f_{1v}f_{2u})}}{2d_\Omega}, \tag{53}$$

and,

$$R = \frac{(d_\Omega f_{1u} + f_{2v}) + \sqrt{(d_\Omega f_{1u} + f_{2v})^2 - 4d_\Omega(f_{1u}f_{2v} - f_{1v}f_{2u})}}{2d_\Omega}, \tag{54}$$

respectively. Therefore, for sufficient condition to exist for diffusion-driven instability, the excitable modes must exist and belong to the interval (52).

Consider the one-dimensional case, the eigenvalues are $k_l^2 = l^2\pi^2$. In order to find the excitable wavenumbers, in addition to the necessary conditions (49), (50), (51) and (52), one requires the sufficient condition of the form

$$k_{l-1}^2 < k_-^2 < k_l^2 < k_+^2 < k_{l+1}^2. \tag{55}$$

Figure 3 represents the real part of the larger eigenvalue as a function of k^2. In Figure 5 the parameter $d_\Omega = 10$ was fixed and the value of γ_Ω was varied, which suggested that when $\gamma_\Omega = 15$ and $\gamma_\Omega = 60$ then no wavenumber excited, however if $\gamma_\Omega,, = 30$ and $\gamma_\Omega = 90$ then only one wavenumber is excited for each value which are k_1^2 and k_2^2 respectively, with $k_1 = \pi$ and $k_2 = 2\pi$. For $\gamma_\Omega = 187$, there are two excitable wavenumbers which are of the form $k_2^2 = (2\pi)^2$ and $k_3^2 = (3\pi)^2$.

A similar approach is applied to the case in two dimensions. The values of d_Ω and γ_Ω are computed. We are interested in finding combination of d_Ω and γ_Ω, such that the curve $\mathrm{Re}(\lambda(k^2))$ encapsulates only one excitable wavenumber. The algorithm is outlined through the following steps:

- Define $d_\Omega = d_c + \epsilon$ where $0 < \epsilon \ll 1$ and $d_c = 8.5676$.
- Compute k_-^2 and k_+^2.
- If $k_{l,m}^2 > k_+^2$ as shown in figure 4 then increase the value of γ_Ω by 1, till the curve includes the wavenumber by shifting to the right.
- If $k_{l,m}^2 < k_-^2$ then decrease the value of γ_Ω by 1, till the curve includes the wavenumber by shifting to the left.
- If there exist two excitable wavenumbers as shown in Figure 5(a) then we decrease ϵ till we obtain a unique excitable wavenumber as shown in figure 5(b).

A similar procedure may be employed to extract excitable wavenumbers from the spectrum of Laplace-Beltrami operator as a sufficient condition for Turing pattern to be formed on the surface.

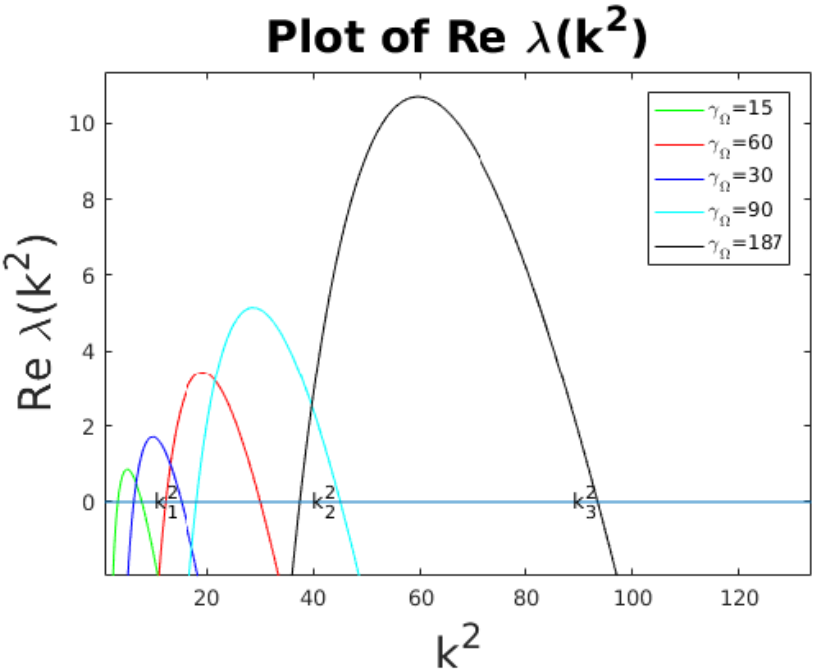

Fig. 3: The plot of the real part of eigenvalue $\lambda(k^2)$ as a function of k^2. For fixed $d_\Omega = 10$ and increasing γ_Ω, we see that when $\gamma_\Omega = 30$ there is only one wavenumber excited ($k_1^2 = \pi^2$), when $\gamma_\Omega = 90$ there is only one wavenumber excited ($k_2^2 = (2\pi)^2$). There are two excitable wavenumbers namely $k_2^2 = (2\pi)^2$ and $k_3^2 = (3\pi)^2$ when $\gamma_\Omega = 187$.

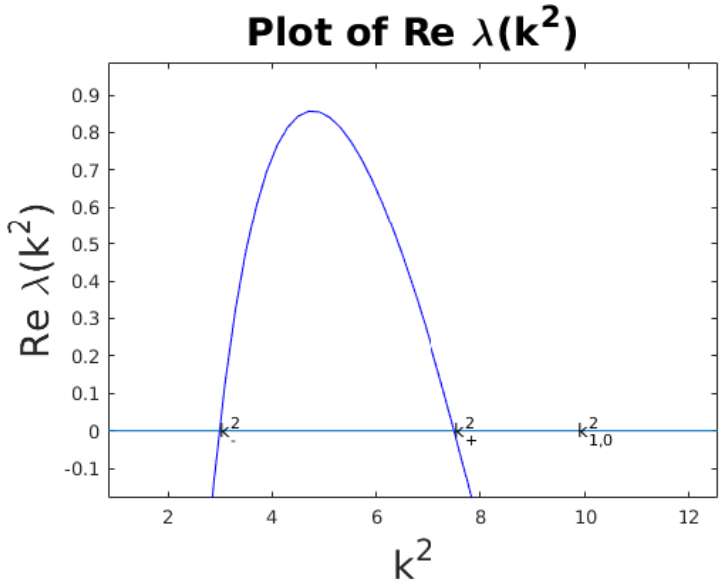

Fig. 4: The plot of the real part of eigenvalue $\lambda(k^2)$ as a function of k^2. For all parameter values suitable for diffusion-driven instability, d_Ω and γ_Ω are varied to capture the excitable wavenumber.

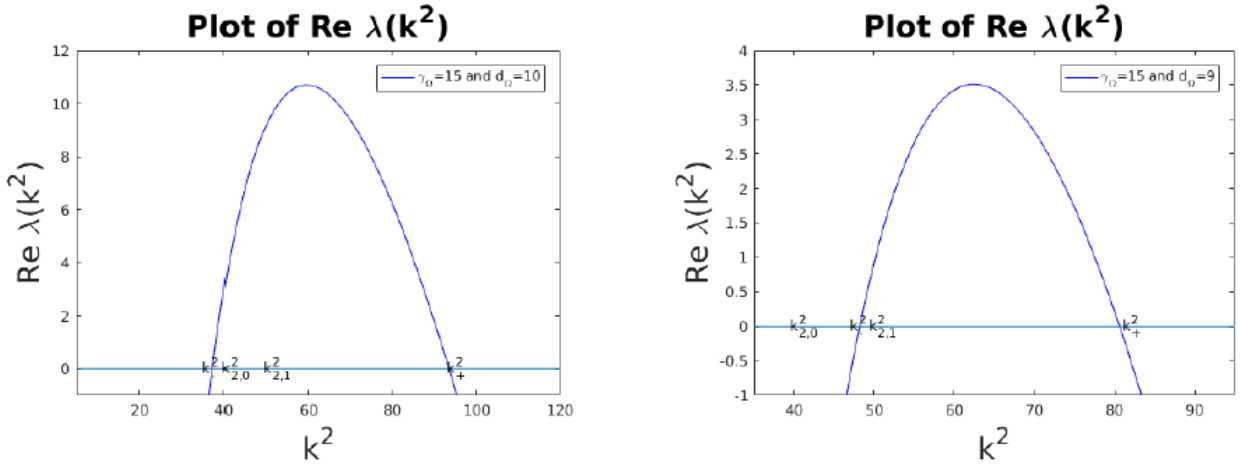

(a) **(b)**

Fig. 5: Plot of the real part of eigenvalue λ(k²) as a function of k², where we see that in figure 5(a) there exist two excitable wavenumbers. By decreasing ϵ we extract a unique excitable wavenumber shown in figure 5(b).

3.3 Turing (parameters) space on the surface

The Turing (parameters) spaces for equations posed on the surface, the conditions for these are obtained in section 2 and outlined as

$$f_{3r} + f_{4s} < 0, \tag{56}$$

$$f_{3r}f_{4s} - f_{3s}f_{4r} > 0, \tag{57}$$

$$d_\Gamma f_{3r} + f_{4s} > 0 \quad \text{and} \quad [d_\Gamma f_{3r} + f_{4s}]^2 - 4d_\Gamma(f_{3r}f_{4s} - f_{3s}f_{4r}) > 0. \tag{58}$$

The parameter spaces are derived on the actual positive real parameter plane (a_2, b_2), for two choices of diffusion ratios namely $d_\Gamma = 20$ and $d_\Gamma = 30$.

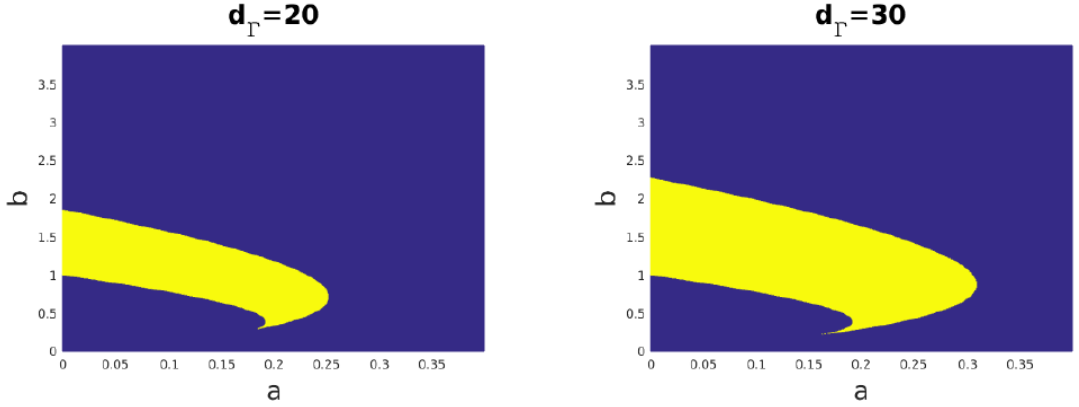

Fig. 6: Turing space for Schnakenberg model for different values of d_Γ: Unstable region is shown in the parameter space (yellow region)

3.4 Turing spaces in the bulk and on the surface

The following sub-figures show diffusion-driven instability spaces for the conditions on diffusion-driven instability given by (35)-(40) in the bulk and on the surface. We combine the Turing spaces (more than one space) in the bulk and on the surface together. We note that if d_Ω is chosen the same as d_Γ, there is no difference in the region corresponding to Turing space as shown in Sub-figure 8(a). In Sub-figures 8(b) and 8(c), it can be seen that for larger values of the diffusion coefficient the Turing space is significantly larger than that for the smaller value of the diffusion coefficient. In the context of pattern formation it, means that regions corresponding to diffusion driven instability enlarge with an increase in the diffusion coefficient.

4. FEM FOR REACTION-DIFFUSION EQUATIONS ON STATIONARY VOLUMES

This section serves to provide the theoretical formulation required to obtain numerical solutions through the finite element method for the system that was explored in section 2. The Sobolev and Hilbert function spaces are the basis used to obtain the weak formulation. The methods of space and time discretisations were investigated and also the time-stepping schemes. We present the weak formulation with the corresponding finite element formulation through a fully implicit treatment by employing the extended form of Newton's method for vector valued functions.

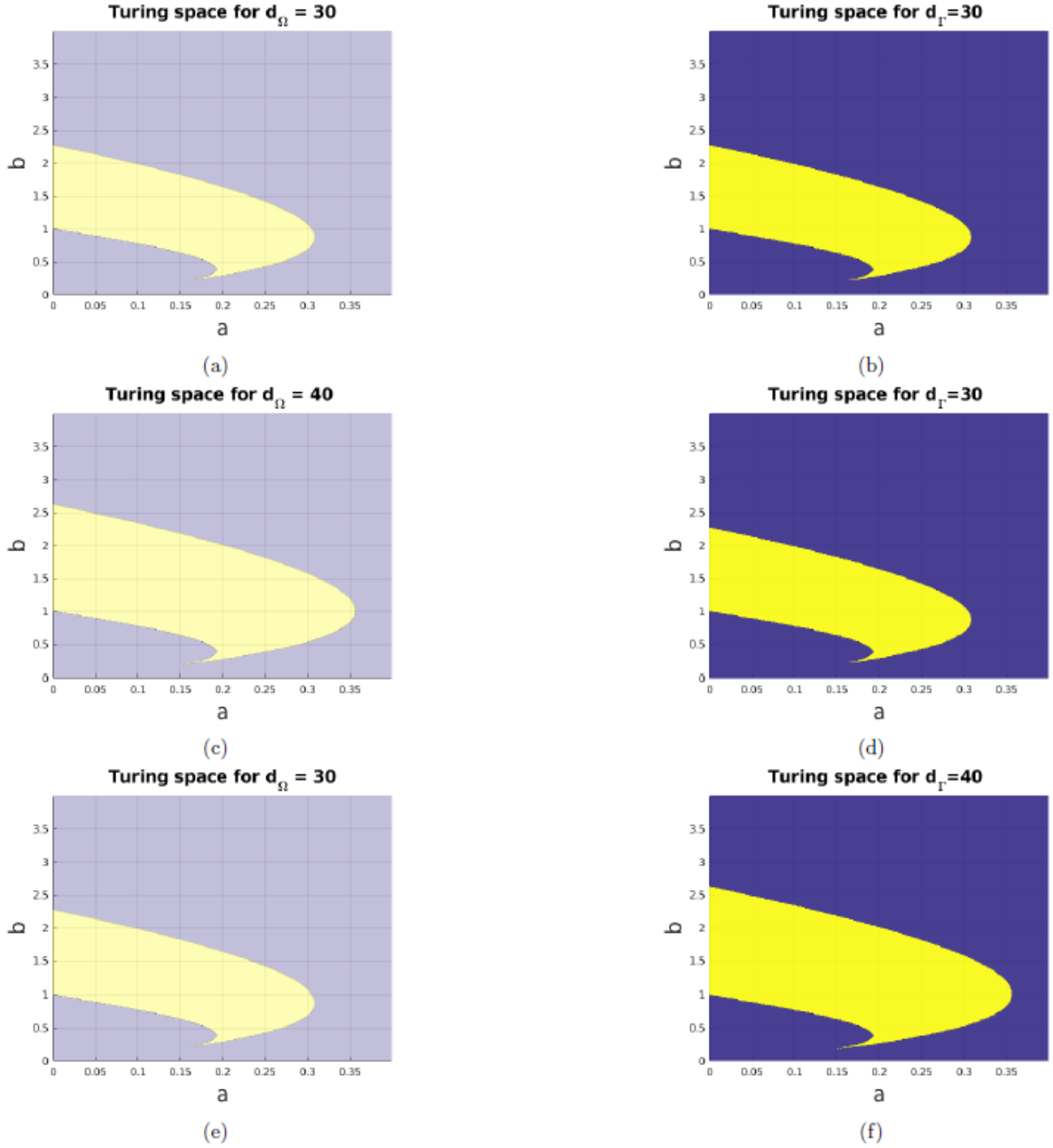

Fig. 7: First row shows that the Turing space for both the bulk and the surface separately for parameter choices $d_\Gamma = 30$ and $d_\Omega = 30$ respectively. Second and third rows show that the Turing space in the bulk and on the surface separately with different parameter choices (second row $d_\Gamma = 30$ and $d_\Omega = 40$) and (third row $d_\Gamma = 30$ and $d_\Omega = 40$)

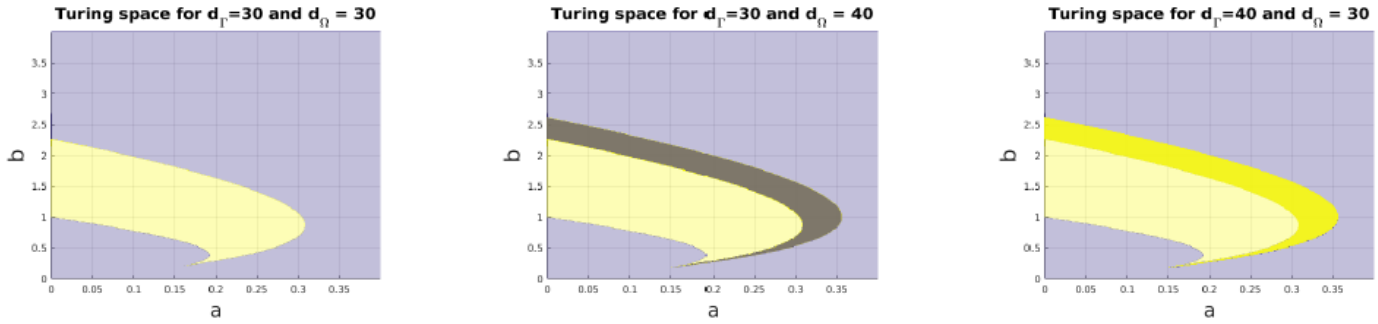

Fig. 8: Sub-figure (a) shows that the Turing space for both the bulk and the surface (cream colour) is shown to exactly coincide for parameter choices $d_\Gamma = 30$ and $d_\Omega = 30$. Sub-figure (b) shows that the Turing space on the surface (cream colour) forms a proper subset of those derived for the bulk equations (union of cream and grey regions) when $d_\Gamma = 30$ and $d_\Omega = 40$. Sub-figure (c) shows that the Turing space for equations on the surface (union of yellow and cream colour regions) with $d_\Gamma = 40$ produces larger region, which contains the spaces for the bulk equation with $d_\Omega = 30$ as proper subset, upon submerging

4.1 Weak formulation

In order to derive the weak formulation, we multiply (13) by a test function say $\varphi \in H^1(\Omega)$ for the bulk and $\psi \in H^1(\Gamma)$ for the surface and integrate over Ω for the bulk and over Γ for the surface written as:

$$\int_\Omega \frac{\partial u}{\partial t}\varphi \, \mathrm{d}\Omega - \int_\Omega \Delta u\varphi \, \mathrm{d}\Omega = \gamma_\Omega \int_\Omega [a_2 - u + u^2 v]\varphi \, \mathrm{d}\Omega,$$

$$\int_\Omega \frac{\partial v}{\partial t}\varphi \, \mathrm{d}\Omega - \int_\Omega d_\Omega \Delta v\varphi \, \mathrm{d}\Omega = \gamma_\Omega \int_\Omega [b_2 - u^2 v]\varphi \, \mathrm{d}\Omega, \qquad \text{in } \Omega \times (0,T]$$

$$\int_\Gamma \frac{\partial r}{\partial t}\psi \, \mathrm{d}\Gamma - \int_\Gamma \Delta_\Gamma r\psi \, \mathrm{d}\Gamma = \gamma_\Gamma \int_\Gamma [a_2 - r + r^2 s - \rho_3 r + \mu u + \delta_2 v]\psi \, \mathrm{d}\Gamma,$$

$$\int_\Gamma \frac{\partial s}{\partial t}\psi \, \mathrm{d}\Gamma - \int_\Gamma d_\Gamma \Delta_\Gamma s\psi \, \mathrm{d}\Gamma = \gamma_\Gamma \int_\Gamma [b_2 - r^2 s - \rho_4 s + \mu_1 u + \delta_3 v]\psi \, \mathrm{d}\Gamma, \quad \text{on } \Gamma \times (0,T].$$

Using the Green's formula for the second terms in the above with the boundary conditions (14), we obtain

$$\begin{aligned}
\int_\Omega \frac{\partial u}{\partial t}\varphi \, \mathrm{d}\Omega + \int_\Omega \nabla u \cdot \nabla\varphi \, \mathrm{d}\Omega &= \gamma_\Omega \int_\Omega [a_2 - u + u^2 v]\varphi \, \mathrm{d}\Omega \\
&\quad + \gamma_\Gamma \int_\Gamma (\rho_3 r - \mu u - \delta_2 v)\varphi \, \mathrm{d}\Gamma, \\
\int_\Omega \frac{\partial v}{\partial t}\varphi \, \mathrm{d}\Omega + d_\Omega \int_\Omega \nabla v \cdot \nabla\varphi \, \mathrm{d}\Omega &= \gamma_\Omega \int_\Omega [b_2 - u^2 v]\varphi \, \mathrm{d}\Omega \\
&\quad + \gamma_\Gamma \int_\Gamma (\rho_4 s - \mu_1 u - \delta_3 v)\varphi \, \mathrm{d}\Gamma, \quad \text{in } \Omega \times (0,T] \\
\int_\Gamma \frac{\partial r}{\partial t}\psi \, \mathrm{d}\Gamma + \int_\Gamma \nabla_\Gamma r \cdot \nabla_\Gamma\psi \, \mathrm{d}\Gamma &= \gamma_\Gamma \int_\Gamma [a_2 - r + r^2 s - \rho_3 r + \mu u + \delta_2 v]\psi \, \mathrm{d}\Gamma, \\
\int_\Gamma \frac{\partial s}{\partial t}\psi \, \mathrm{d}\Gamma + d_\Gamma \int_\Gamma \nabla_\Gamma s \cdot \nabla_\Gamma\psi \, \mathrm{d}\Gamma &= \gamma_\Gamma \int_\Gamma [b_2 - r^2 s - \rho_4 s + \mu_1 u + \delta_3 v]\psi \, \mathrm{d}\Gamma, \text{on } \Gamma \times (0,T].
\end{aligned}$$

4.2 Spatial discretisation of the weak formulation

We discretise the original domain Ω and its boundary Γ to obtain Ω_h and Γ_h where $\Omega_h \subset \Omega$ and $\Gamma_h \subset \Gamma$ with N_Ω and N_Γ the number of vertices associated to their respective discretisation. Let V_{Ω_h} and V_{Γ_h} denote the finite element function spaces associated to the discretised domains Ω_h and Γ_h respectively. The finite element formulation is then to seek $u_h, v_h \in V_{\Omega_h}$ and $r_h, s_h \in V_{\Gamma_h}$ such that for $t > 0$ the equations

$$\begin{aligned}
\int_{\Omega_h} \frac{\partial u_h}{\partial t}\varphi_h \, \mathrm{d}\Omega_h + \int_{\Omega_h} \nabla u_h \cdot \nabla\varphi_h \, \mathrm{d}\Omega_h &= \gamma_\Omega \int_{\Omega_h} [a_2 - u_h + u_h^2 v_h]\varphi_h \, \mathrm{d}\Omega_h \\
&\quad + \gamma_\Gamma \int_{\Gamma_h} (\rho_3 r_h - \mu u_h - \delta_2 v_h)\varphi_h \, \mathrm{d}\Gamma_h, \\
\int_{\Omega_h} \frac{\partial v_h}{\partial t}\varphi_h \, \mathrm{d}\Omega_h + d_\Omega \int_{\Omega_h} \nabla v_h \cdot \nabla\varphi_h \, \mathrm{d}\Omega_h &= \gamma_\Omega \int_{\Omega_h} [b_2 - u_h^2 v_h]\varphi_h \, \mathrm{d}\Omega_h \\
&\quad + \gamma_\Gamma \int_{\Gamma_h} (\rho_4 s_h - \mu_1 u_h - \delta_3 v_h)\varphi_h \, \mathrm{d}\Gamma_h,
\end{aligned}$$

$$\int_{\Gamma_h} \frac{\partial r_h}{\partial t}\psi_h \, \mathrm{d}\Gamma_h + \int_{\Gamma_h} \nabla_\Gamma r_h \cdot \nabla_\Gamma \psi_h \, \mathrm{d}\Gamma_h = \gamma_\Gamma \int_{\Gamma_h} [a_2 - r_h + r_h^2 s_h - \rho_3 r_h + \mu u_h + \delta_2 v_h]\psi_h \, \mathrm{d}\Gamma_h,$$

$$\int_{\Gamma_h} \frac{\partial s_h}{\partial t}\psi_h \, \mathrm{d}\Gamma_h + d_\Gamma \int_{\Gamma_h} \nabla_\Gamma s_h \cdot \nabla_\Gamma \psi_h \, \mathrm{d}\Gamma_h = \gamma_\Gamma \int_{\Gamma_h} [b_2 - r_h^2 s_h - \rho_4 s_h + \mu_1 u_h + \delta_3 v_h]\psi_h \, \mathrm{d}\Gamma_h,$$

are true for all test functions $\varphi_h \in V_{\Omega_h}$ and $\psi_h \in V_{\Gamma_h}$ respectively. Let $\{\varphi_i\}_{i=1}^{N_\Omega}$ and $\{\psi_i\}_{i=1}^{N_\Gamma}$ be the set of piecewise bilinear basis functions. It is known that the spaces V_{Ω_h} and V_{Γ_h} are spanned by the basis functions $\{\varphi_i\}_{i=1}^{N_\Omega}$ and $\{\psi_i\}_{i=1}^{N_\Gamma}$ respectively [36]. Thus, u_h, v_h, r_h and s_h may be expanded in terms of linear combinations of its corresponding basis functions namely $\{\varphi_i\}_{i=1}^{N_\Omega}$ and $\{\psi_i\}_{i=1}^{N_\Gamma}$. Substituting the expressions $u_h = \sum_{i=1}^{N_\Omega} U_i \, \varphi_i$, $v_h = \sum_{i=1}^{N_\Omega} V_i \, \varphi_i$, $r_h = \sum_{i=1}^{N_\Gamma} R_i \, \psi_i$, and $s_h = \sum_{i=1}^{N_\Gamma} S_i \, \psi_i$ in the finite element formulations leads to a system of differential equations written in matrix, notation as:

$$\begin{aligned}
M_0\mathbf{U_t} + \gamma_\Omega M_0\mathbf{U} + A_0\mathbf{U} \quad & -\gamma_\Omega B_0(\mathbf{U},\mathbf{V})\mathbf{U} \\
& -\gamma_\Gamma(\rho_3 M_{10}\mathbf{R} - \mu M_{00}\mathbf{U} - \delta_2 M_{00}\mathbf{V}) = \gamma_\Omega a_2 \mathbf{C_0}, \\
M_0\mathbf{V_t} + d_\Omega A_0\mathbf{V} + \gamma_\Omega B_0 \quad & (\mathbf{U},\mathbf{U})\mathbf{V} \\
& -\gamma_\Gamma(\rho_4 M_{10}\mathbf{S} - \mu_1 M_{00}\mathbf{U} - \delta_3 M_{00}\mathbf{V}) = \gamma_\Omega b_2 \mathbf{C_0}, \\
M_1\mathbf{R_t} + \gamma_\Gamma M_1\mathbf{R} + A_1\mathbf{R} \quad & -\gamma_\Gamma B_1(\mathbf{R},\mathbf{S})\mathbf{R} \\
& +\gamma_\Gamma(\rho_3 M_{11}\mathbf{R} - \mu M_{01}\mathbf{U} - \delta_2 M_{01}\mathbf{V}) = \gamma_\Gamma a_2 \mathbf{C_1}, \\
M_1\mathbf{S_t} + d_\Gamma A_1\mathbf{S} + \gamma_\Gamma B_1 \quad & (\mathbf{R},\mathbf{R})\mathbf{S} \\
& +\gamma_\Gamma(\rho_4 M_{11}\mathbf{S} - \mu_1 M_{01}\mathbf{U} - \delta_3 M_{01}\mathbf{V}) = \gamma_\Gamma a_2 \mathbf{C_1},
\end{aligned}$$

Where the matrices with their corresponding entries are given by:

$$\begin{aligned}
(M_0)_{ij} &= \int_{\Omega_h} \varphi_i \, \varphi_j \mathrm{d}\Omega_h, \quad (A_0)_{ij} = \int_{\Omega_h} \nabla \varphi_i \cdot \nabla \varphi_j \mathrm{d}\Omega_h, \quad \mathbf{C_0} = \int_{\Omega_h} \varphi_j \, \mathrm{d}\Omega_h, \\
(B_0(\mathbf{U},\mathbf{V}))_{ij} &= \int_{\Omega_h} (U_i\varphi_i)(V_i\varphi_i)\varphi_i\varphi_j \mathrm{d}\Omega_h, \quad (B_0(\mathbf{U},\mathbf{U}))_{ij} = \int_{\Omega_h} (U_i\varphi_i)(U_i\varphi_i)\varphi_i\varphi_j \mathrm{d}\Omega_h,
\end{aligned}$$

And the entries for $M_1, A_1, B_1(\mathbf{R},\mathbf{S})$ and $\mathbf{C_1}$, are expressed in similar way to those expressed for matrices with subscript 0. The entries of the matrices that are constructed from the combination of function spaces defined in the bulk and on the surface are defined by

$$\begin{aligned}
(M_{10})_{ij} &= \int_{\Gamma_h} \psi_i \, \varphi_j \mathrm{d}\Gamma_h, \quad (M_{01})_{ij} = \int_{\Gamma_h} \varphi_i \, \psi_j \mathrm{d}\Gamma_h, \\
(M_{00})_{ij} &= \int_{\Gamma_h} \varphi_i \, \varphi_j \mathrm{d}\Gamma_h, \quad (M_{11})_{ij} = \int_{\Gamma_h} \psi_i \, \psi_j \mathrm{d}\Gamma_h,
\end{aligned}$$

Where M is the mass matrix and A is the stiffness matrix, B is the matrix corresponding to the non-linear terms and $\mathbf{C}$ is the column vector.

4.3 Mesh generation (using deal.II) [37]

The usual approach to discretising Ω and Γ is such that, Ω is first discretised and denoted by Ω_h. The union of those elements from Ω_h whose vertices lie on $\partial\Omega$ is considered as the discretisation of Γ, which is denoted by Γ_h. Bulk is discretised by quadrilateral elements each with uniform structure throughout Ω_h. Triangulation Γ_h is also a uniform set of 2-dimensional quadrilaterals consisting of the external faces of all the bulk elements that have at least one vertex on Γ_h.

4.4. Time discretisation

We discretise the time interval $[0,T]$ into a finite number of uniform subintervals such that $0 = t_0 < t_1 \cdots < t_J = T$. Let τ be the time steps and J be a fixed positive integer, then $T = J\tau$. We denote the approximate solution at time $t_n = the\ the\ n\tau$ by $u_h^n = u_h(.,t_n)$ where $n = 0,1,\cdots,J$ and similar for the other variables. A fully implicit Euler scheme is used to solve the system in time. The fully implicit scheme is applied to the uniform time discretisation. We can obtain the fully discretised system as

$$\begin{aligned}
M_0\frac{\mathbf{U}^n - \mathbf{U}^{n-1}}{\tau} + \gamma_\Omega M_0\mathbf{U}^n \quad & +A_0\mathbf{U}^n - \gamma_\Omega B_0(\mathbf{U}^n,\mathbf{V}^n)\mathbf{U}^n \\
& -\gamma_\Gamma(\rho_3 M_{10}\mathbf{R}^n - \mu M_{00}\mathbf{U}^n - \delta_2 M_{00}\mathbf{V}^n) = \gamma_\Omega a_2 \mathbf{C_0}, \\
M_0\frac{\mathbf{V}^n - \mathbf{V}^{n-1}}{\tau} + d_\Omega A_0\mathbf{V}^n \quad & +\gamma_\Omega B_0(\mathbf{U}^n,\mathbf{U}^n)\mathbf{V}^n \\
& -\gamma_\Gamma(\rho_4 M_{10}\mathbf{S}^n - \mu_1 M_{00}\mathbf{U}^n - \delta_3 M_{00}\mathbf{V}^n) = \gamma_\Omega b_2 \mathbf{C_0}, \\
M_1\frac{\mathbf{R}^n - \mathbf{R}^{n-1}}{\tau} + \gamma_\Gamma M_1\mathbf{R}^n \quad & +A_1\mathbf{R}^n - \gamma_\Gamma B_1(\mathbf{R}^n,\mathbf{S}^n)\mathbf{R}^n \\
& +\gamma_\Gamma(\rho_3 M_{11}\mathbf{R}^n - \mu M_{01}\mathbf{U}^n - \delta_2 M_{01}\mathbf{V}^n) = \gamma_\Gamma a_2 \mathbf{C_1}, \\
M_1\frac{\mathbf{S}^n - \mathbf{S}^{n-1}}{\tau} + d_\Gamma A_1\mathbf{S}^n \quad & +\gamma_\Gamma B_1(\mathbf{R}^n,\mathbf{R}^n)\mathbf{S}^n \\
& +\gamma_\Gamma(\rho_4 M_{11}\mathbf{S}^n - \mu_1 M_{01}\mathbf{U}^n - \delta_3 M_{01}\mathbf{V}^n) = \gamma_\Gamma b_2 \mathbf{C_1}.
\end{aligned}$$

Algebraic manipulation and rearrangement of each equation leads to writing the system in a different form which is

$$\begin{aligned}\mathbf{F_1}(\mathbf{U}^n,\mathbf{V}^n,\mathbf{R}^n,\mathbf{S}^n) &= 0,\\ \mathbf{F_2}(\mathbf{U}^n,\mathbf{V}^n,\mathbf{R}^n,\mathbf{S}^n) &= 0,\\ \mathbf{F_3}(\mathbf{U}^n,\mathbf{V}^n,\mathbf{R}^n,\mathbf{S}^n) &= 0,\\ \mathbf{F_4}(\mathbf{U}^n,\mathbf{V}^n,\mathbf{R}^n,\mathbf{S}^n) &= 0,\end{aligned}$$

Where

$$\begin{aligned}\mathrm{F}_1(\mathrm{U}^n,\mathrm{V}^n,\mathrm{R}^n,\mathrm{S}^n) &= \left(\left(\frac{1}{\tau}+\gamma_\Omega\right)M_0+A_0\right)U^n-\gamma_\Omega B_0(\mathrm{U}^n,\mathrm{V}^n)\mathrm{U}^n-\gamma_\Gamma(\rho_3 M_{10}\mathrm{R}^n-\mu M_{00}\mathrm{U}^n-\delta_2 M_{00}\mathrm{V}^n)-\gamma_\Omega a_2\mathrm{C}_0-\frac{1}{\tau}M_0\mathrm{U}^{n-1},\\ \mathrm{F}_2(\mathrm{U}^n,\mathrm{V}^n,\mathrm{R}^n,\mathrm{S}^n) &= \left(\frac{1}{\tau}M_0+d_\Omega A_0\right)V^n-\gamma_\Omega B_0(\mathrm{U}^n,\mathrm{U}^n)\mathrm{V}^n-\gamma_\Gamma(\rho_4 M_{10}\mathrm{S}^n-\mu_1 M_{00}\mathrm{U}^n-\delta_3 M_{00}\mathrm{V}^n)-\gamma_\Omega b_2\mathrm{C}_0-\frac{1}{\tau}M_0\mathrm{V}^{n-1},\\ \mathrm{F}_3(\mathrm{U}^n,\mathrm{V}^n,\mathrm{R}^n,\mathrm{S}^n) &= \left(\left(\frac{1}{\tau}+\gamma_\Gamma\right)M_1+A_1\right)R^n-\gamma_\Gamma B_1(\mathrm{R}^n,\mathrm{S}^n)\mathrm{R}^n-\gamma_\Gamma(\rho_3 M_{11}\mathrm{R}^n-\mu M_{01}\mathrm{U}^n-\delta_2 M_{01}\mathrm{V}^n)-\gamma_\Gamma a_2\mathrm{C}_1-\frac{1}{\tau}M_1\mathrm{R}^{n-1},\\ \mathrm{F}_4(\mathrm{U}^n,\mathrm{V}^n,\mathrm{R}^n,\mathrm{S}^n) &= \left(\frac{1}{\tau}M_1+d_\Gamma A_1\right)S^n-\gamma_\Gamma B_1(\mathrm{R}^n,\mathrm{R}^n)\mathrm{S}^n-\gamma_\Gamma(\rho_4 M_{11}\mathrm{S}^n-\mu_1 M_{01}\mathrm{U}^n-\delta_3 M_{01}\mathrm{V}^n)-\gamma_\Gamma b_2\mathrm{C}_1-\frac{1}{\tau}M_1\mathrm{S}^{n-1},\end{aligned}$$

In order to solve the system of non-linear equations, the employing the extended form of Newton's method for vector valued functions leads to write

$$\mathbf{J}_{\mathbf{F}_\iota}\big|_{(\mathbf{u}_k^n,\mathbf{v}_k^n,\mathbf{r}_k^n,\mathbf{s}_k^n)}(\mathbf{u}_{k+1}^n-\mathbf{u}_k^n,\mathbf{v}_{k+1}^n-\mathbf{v}_k^n,\mathbf{r}_{k+1}^n-\mathbf{r}_k^n,\mathbf{s}_{k+1}^n-\mathbf{s}_k^n)=-\mathbf{F}_\iota(\mathbf{u}_k^n,\mathbf{v}_k^n,\mathbf{r}_k^n,\mathbf{s}_k^n), \tag{59}$$

Where the index $\iota = 1,2,3,4$ and

$$\mathbf{J}_{\mathbf{F}}\big|_{(\mathbf{u}_k^n,\mathbf{v}_k^n,\mathbf{r}_k^n,\mathbf{s}_k^n)}=\begin{pmatrix}\frac{\partial\mathbf{F}_1(\mathbf{u}_k^n,\mathbf{v}_k^n,\mathbf{r}_k^n,\mathbf{s}_k^n)}{\partial\mathbf{u}_k^n} & \frac{\partial\mathbf{F}_1(\mathbf{u}_k^n,\mathbf{v}_k^n,\mathbf{r}_k^n,\mathbf{s}_k^n)}{\partial\mathbf{v}_k^n} & \frac{\partial\mathbf{F}_1(\mathbf{u}_k^n,\mathbf{v}_k^n,\mathbf{r}_k^n,\mathbf{s}_k^n)}{\partial\mathbf{r}_k^n} & \frac{\partial\mathbf{F}_1(\mathbf{u}_k^n,\mathbf{v}_k^n,\mathbf{r}_k^n,\mathbf{s}_k^n)}{\partial\mathbf{s}_k^n}\\ \frac{\partial\mathbf{F}_2(\mathbf{u}_k^n,\mathbf{v}_k^n,\mathbf{r}_k^n,\mathbf{s}_k^n)}{\partial\mathbf{u}_k^n} & \frac{\partial\mathbf{F}_2(\mathbf{u}_k^n,\mathbf{v}_k^n,\mathbf{r}_k^n,\mathbf{s}_k^n)}{\partial\mathbf{v}_k^n} & \frac{\partial\mathbf{F}_2(\mathbf{u}_k^n,\mathbf{v}_k^n,\mathbf{r}_k^n,\mathbf{s}_k^n)}{\partial\mathbf{r}_k^n} & \frac{\partial\mathbf{F}_2(\mathbf{u}_k^n,\mathbf{v}_k^n,\mathbf{r}_k^n,\mathbf{s}_k^n)}{\partial\mathbf{s}_k^n}\\ \frac{\partial\mathbf{F}_3(\mathbf{u}_k^n,\mathbf{v}_k^n,\mathbf{r}_k^n,\mathbf{s}_k^n)}{\partial\mathbf{u}_k^n} & \frac{\partial\mathbf{F}_3(\mathbf{u}_k^n,\mathbf{v}_k^n,\mathbf{r}_k^n,\mathbf{s}_k^n)}{\partial\mathbf{v}_k^n} & \frac{\partial\mathbf{F}_3(\mathbf{u}_k^n,\mathbf{v}_k^n,\mathbf{r}_k^n,\mathbf{s}_k^n)}{\partial\mathbf{r}_k^n} & \frac{\partial\mathbf{F}_3(\mathbf{u}_k^n,\mathbf{v}_k^n,\mathbf{r}_k^n,\mathbf{s}_k^n)}{\partial\mathbf{s}_k^n}\\ \frac{\partial\mathbf{F}_4(\mathbf{u}_k^n,\mathbf{v}_k^n,\mathbf{r}_k^n,\mathbf{s}_k^n)}{\partial\mathbf{u}_k^n} & \frac{\partial\mathbf{F}_4(\mathbf{u}_k^n,\mathbf{v}_k^n,\mathbf{r}_k^n,\mathbf{s}_k^n)}{\partial\mathbf{v}_k^n} & \frac{\partial\mathbf{F}_4(\mathbf{u}_k^n,\mathbf{v}_k^n,\mathbf{r}_k^n,\mathbf{s}_k^n)}{\partial\mathbf{r}_k^n} & \frac{\partial\mathbf{F}_4(\mathbf{u}_k^n,\mathbf{v}_k^n,\mathbf{r}_k^n,\mathbf{s}_k^n)}{\partial\mathbf{s}_k^n}\end{pmatrix}, \tag{60}$$

and the entries of $\mathbf{J_F}$ are expressed by:

$$\begin{aligned}\frac{\partial\mathbf{F}_1(\mathbf{u}_k^n,\mathbf{v}_k^n,\mathbf{r}_k^n,\mathbf{s}_k^n)}{\partial\mathbf{u}_k^n} &= (\frac{1}{\tau}+\gamma_\Omega)M_0+A_0-2\gamma_\Omega B_0(\mathbf{u}_k^n,\mathbf{v}_k^n)+\gamma_\Gamma\mu M_{00},\\ \frac{\partial\mathbf{F}_1(\mathbf{u}_k^n,\mathbf{v}_k^n,\mathbf{r}_k^n,\mathbf{s}_k^n)}{\partial\mathbf{v}_k^n} &= -\gamma_\Omega B_0(\mathbf{u}_k^n,\mathbf{u}_k^n)+\gamma_\Gamma\delta_2 M_{00},\\ \frac{\partial\mathbf{F}_1(\mathbf{u}_k^n,\mathbf{v}_k^n,\mathbf{r}_k^n,\mathbf{s}_k^n)}{\partial\mathbf{r}_k^n} &= -\gamma_\Gamma\rho_3 M_{10},\\ \frac{\partial\mathbf{F}_1(\mathbf{u}_k^n,\mathbf{v}_k^n,\mathbf{r}_k^n,\mathbf{s}_k^n)}{\partial\mathbf{s}_k^n} &= 0,\\ \frac{\partial\mathbf{F}_2(\mathbf{u}_k^n,\mathbf{v}_k^n,\mathbf{r}_k^n,\mathbf{s}_k^n)}{\partial\mathbf{u}_k^n} &= 2\gamma_\Omega B_0(\mathbf{u}_k^n,\mathbf{v}_k^n)+\gamma_\Gamma\mu_1 M_{00},\\ \frac{\partial\mathbf{F}_2(\mathbf{u}_k^n,\mathbf{v}_k^n,\mathbf{r}_k^n,\mathbf{s}_k^n)}{\partial\mathbf{v}_k^n} &= \frac{1}{\tau}M_0+d_\Omega A_0+\gamma_\Omega B_0(\mathbf{u}_k^n,\mathbf{u}_k^n)+\gamma_\Gamma\delta_3 M_{00},\\ \frac{\partial\mathbf{F}_2(\mathbf{u}_k^n,\mathbf{v}_k^n,\mathbf{r}_k^n,\mathbf{s}_k^n)}{\partial\mathbf{r}_k^n} &= 0,\\ \frac{\partial\mathbf{F}_2(\mathbf{u}_k^n,\mathbf{v}_k^n,\mathbf{r}_k^n,\mathbf{s}_k^n)}{\partial\mathbf{s}_k^n} &= -\gamma_\Gamma\rho_4 M_{10},\\ \frac{\partial\mathbf{F}_3(\mathbf{u}_k^n,\mathbf{v}_k^n,\mathbf{r}_k^n,\mathbf{s}_k^n)}{\partial\mathbf{u}_k^n} &= -\gamma_\Gamma\mu M_{01},\\ \frac{\partial\mathbf{F}_3(\mathbf{u}_k^n,\mathbf{v}_k^n,\mathbf{r}_k^n,\mathbf{s}_k^n)}{\partial\mathbf{v}_k^n} &= -\gamma_\Gamma\delta_2 M_{01},\\ \frac{\partial\mathbf{F}_3(\mathbf{u}_k^n,\mathbf{v}_k^n,\mathbf{r}_k^n,\mathbf{s}_k^n)}{\partial\mathbf{r}_k^n} &= (\frac{1}{\tau}+\gamma_\Gamma)M_1+A_1-2\gamma_\Gamma B_1(\mathbf{r}_k^n,\mathbf{s}_k^n)+\gamma_\Gamma\rho_3 M_{11},\\ \frac{\partial\mathbf{F}_3(\mathbf{u}_k^n,\mathbf{v}_k^n,\mathbf{r}_k^n,\mathbf{s}_k^n)}{\partial\mathbf{s}_k^n} &= -\gamma_\Gamma B_1(\mathbf{r}_k^n,\mathbf{r}_k^n),\\ \frac{\partial\mathbf{F}_4(\mathbf{u}_k^n,\mathbf{v}_k^n,\mathbf{r}_k^n,\mathbf{s}_k^n)}{\partial\mathbf{u}_k^n} &= -\gamma_\Gamma\mu_1 M_{01},\\ \frac{\partial\mathbf{F}_4(\mathbf{u}_k^n,\mathbf{v}_k^n,\mathbf{r}_k^n,\mathbf{s}_k^n)}{\partial\mathbf{v}_k^n} &= -\gamma_\Gamma\delta_3 M_{01},\\ \frac{\partial\mathbf{F}_4(\mathbf{u}_k^n,\mathbf{v}_k^n,\mathbf{r}_k^n,\mathbf{s}_k^n)}{\partial\mathbf{r}_k^n} &= 2\gamma_\Gamma B_1(\mathbf{r}_k^n,\mathbf{s}_k^n),\\ \frac{\partial\mathbf{F}_4(\mathbf{u}_k^n,\mathbf{v}_k^n,\mathbf{r}_k^n,\mathbf{s}_k^n)}{\partial\mathbf{s}_k^n} &= \frac{1}{\tau}M_1+d_\Gamma A_1+\gamma_\Gamma B_1(\mathbf{r}_k^n,\mathbf{r}_k^n)+\gamma_\Gamma\rho_4 M_{11}.\end{aligned}$$

Substituting (60) in (59) and simplifying, we obtain

$$
\begin{aligned}
&(\mathbf{u}_{k+1}^n) + [-\gamma_\Omega B_0(\mathbf{u}_k^n, \mathbf{u}_k^n)](\mathbf{v}_{k+1}^n) \\
&-\gamma_\Gamma[(\rho_3 M_{10})\mathbf{r}_{k+1}^n - (\mu M_{00})\mathbf{u}_{k+1}^n - (\delta_2 M_{00})\mathbf{v}_{k+1}^n] \\
&= -2\gamma_\Omega B_0(\mathbf{u}_k^n, \mathbf{v}_k^n)\mathbf{u}_k^n + \gamma_\Omega a_2 \mathbf{C_0} + \frac{1}{\tau} M_0 \mathbf{u}^{n-1}, \\
(\mathbf{u}_{k+1}^n) \quad &+[\frac{1}{\tau} M_0 + d_\Omega A_0 + \gamma_\Omega B_0(\mathbf{u}_k^n, \mathbf{u}_k^n)](\mathbf{v}_{k+1}^n) \\
&-\gamma_\Gamma[(\rho_4 M_{10})\mathbf{s}_{k+1}^n - (\mu_1 M_{00})\mathbf{u}_{k+1}^n - (\delta_3 M_{00})\mathbf{u}_{k+1}^n] \\
&= 2\gamma_\Omega B_0(\mathbf{u}_k^n, \mathbf{u}_k^n)\mathbf{v}_k^n + \gamma_\Omega b_2 \mathbf{C_0} + \frac{1}{\tau} M_0 \mathbf{v}^{n-1}, \\
&(\mathbf{r}_{k+1}^n) + [-\gamma_\Gamma B_1(\mathbf{r}_k^n, \mathbf{r}_k^n)](\mathbf{s}_{k+1}^n) \\
&+\gamma_\Gamma[(\rho_3 M_{11})\mathbf{r}_{k+1}^n - (\mu M_{01})\mathbf{u}_{k+1}^n - (\delta_2 M_{01})\mathbf{v}_{k+1}^n] \\
&= -2\gamma_\Gamma B_1(\mathbf{r}_k^n, \mathbf{s}_k^n)\mathbf{r}_k^n + \gamma_\Gamma a_2 \mathbf{C_1} + \frac{1}{\tau} M_1 \mathbf{r}^{n-1}, \\
(\mathbf{r}_{k+1}^n) \quad &+[\frac{1}{\tau} M_1 + d_\Gamma A_1 + \gamma_\Gamma B_1(\mathbf{r}_k^n, \mathbf{r}_k^n)](\mathbf{s}_{k+1}^n) \\
&+\gamma_\Gamma[(\rho_4 M_{11})\mathbf{s}_{k+1}^n - (\mu_1 M_{01})\mathbf{u}_{k+1}^n - (\delta_3 M_{01})\mathbf{v}_{k+1}^n] \\
&= 2\gamma_\Gamma B_1(\mathbf{r}_k^n, \mathbf{r}_k^n)\mathbf{s}_k^n + \gamma_\Gamma b_2 \mathbf{C_1} + \frac{1}{\tau} M_1 \mathbf{s}^{n-1},
\end{aligned}
$$

Which can be written in matrix form as

$$
\begin{pmatrix}
\frac{\partial \mathbf{F}_1(\mathbf{u}_k^n, \mathbf{v}_k^n, \mathbf{r}_k^n, \mathbf{s}_k^n)}{\partial \mathbf{u}_k^n} & \frac{\partial \mathbf{F}_1(\mathbf{u}_k^n, \mathbf{v}_k^n, \mathbf{r}_k^n, \mathbf{s}_k^n)}{\partial \mathbf{v}_k^n} & \frac{\partial \mathbf{F}_1(\mathbf{u}_k^n, \mathbf{v}_k^n, \mathbf{r}_k^n, \mathbf{s}_k^n)}{\partial \mathbf{r}_k^n} & \frac{\partial \mathbf{F}_1(\mathbf{u}_k^n, \mathbf{v}_k^n, \mathbf{r}_k^n, \mathbf{s}_k^n)}{\partial \mathbf{s}_k^n} \\
\frac{\partial \mathbf{F}_2(\mathbf{u}_k^n, \mathbf{v}_k^n, \mathbf{r}_k^n, \mathbf{s}_k^n)}{\partial \mathbf{u}_k^n} & \frac{\partial \mathbf{F}_2(\mathbf{u}_k^n, \mathbf{v}_k^n, \mathbf{r}_k^n, \mathbf{s}_k^n)}{\partial \mathbf{v}_k^n} & \frac{\partial \mathbf{F}_2(\mathbf{u}_k^n, \mathbf{v}_k^n, \mathbf{r}_k^n, \mathbf{s}_k^n)}{\partial \mathbf{r}_k^n} & \frac{\partial \mathbf{F}_2(\mathbf{u}_k^n, \mathbf{v}_k^n, \mathbf{r}_k^n, \mathbf{s}_k^n)}{\partial \mathbf{s}_k^n} \\
\frac{\partial \mathbf{F}_3(\mathbf{u}_k^n, \mathbf{v}_k^n, \mathbf{r}_k^n, \mathbf{s}_k^n)}{\partial \mathbf{u}_k^n} & \frac{\partial \mathbf{F}_3(\mathbf{u}_k^n, \mathbf{v}_k^n, \mathbf{r}_k^n, \mathbf{s}_k^n)}{\partial \mathbf{v}_k^n} & \frac{\partial \mathbf{F}_3(\mathbf{u}_k^n, \mathbf{v}_k^n, \mathbf{r}_k^n, \mathbf{s}_k^n)}{\partial \mathbf{r}_k^n} & \frac{\partial \mathbf{F}_3(\mathbf{u}_k^n, \mathbf{v}_k^n, \mathbf{r}_k^n, \mathbf{s}_k^n)}{\partial \mathbf{s}_k^n} \\
\frac{\partial \mathbf{F}_4(\mathbf{u}_k^n, \mathbf{v}_k^n, \mathbf{r}_k^n, \mathbf{s}_k^n)}{\partial \mathbf{u}_k^n} & \frac{\partial \mathbf{F}_4(\mathbf{u}_k^n, \mathbf{v}_k^n, \mathbf{r}_k^n, \mathbf{s}_k^n)}{\partial \mathbf{v}_k^n} & \frac{\partial \mathbf{F}_4(\mathbf{u}_k^n, \mathbf{v}_k^n, \mathbf{r}_k^n, \mathbf{s}_k^n)}{\partial \mathbf{r}_k^n} & \frac{\partial \mathbf{F}_4(\mathbf{u}_k^n, \mathbf{v}_k^n, \mathbf{r}_k^n, \mathbf{s}_k^n)}{\partial \mathbf{s}_k^n}
\end{pmatrix}
\begin{pmatrix}
\mathbf{u}_{k+1}^n \\ \mathbf{v}_{k+1}^n \\ \mathbf{r}_{k+1}^n \\ \mathbf{s}_{k+1}^n
\end{pmatrix}
$$

$$
= \begin{pmatrix}
-2\gamma_\Omega B_0(\mathbf{u}_k^n, \mathbf{v}_k^n)\mathbf{u}_k^n + \gamma_\Omega a_2 \mathbf{C_0} + \frac{1}{\tau} M_0 \mathbf{u}^{n-1} \\
2\gamma_\Omega B_0(\mathbf{u}_k^n, \mathbf{u}_k^n)\mathbf{v}_k^n + \gamma_\Omega b_2 \mathbf{C_0} + \frac{1}{\tau} M_0 \mathbf{v}^{n-1} \\
-2\gamma_\Gamma B_1(\mathbf{r}_k^n, \mathbf{s}_k^n)\mathbf{r}_k^n + \gamma_\Gamma a_2 \mathbf{C_1} + \frac{1}{\tau} M_1 \mathbf{r}^{n-1} \\
2\gamma_\Gamma B_1(\mathbf{r}_k^n, \mathbf{r}_k^n)\mathbf{s}_k^n + \gamma_\Gamma b_2 \mathbf{C_1} + \frac{1}{\tau} M_1 \mathbf{s}^{n-1}
\end{pmatrix}.
$$

5. NUMERICAL SOLUTION FOR COUPLED BULK-SURFACE REACTION-DIFFUSION EQUATIONS

In this section, we carry out the numerical simulations for the systems that were explored in section 2. We employ a fully implicit time-stepping scheme based on the extended form of Newton's method with the finite element formulation presented in section 4 to proceed with obtaining numerical approximate solutions both in space and in time. We perform the finite element simulations on two types of bulk-surface domains. The first is a cuboid forming the bulk and its six quadrilateral faces forming the corresponding surface. The second domain is a three dimensional ball forming the bulk and hollow sphere bounding the ball forming the corresponding surface.

The finite element library deal.ii [37] is employed to simulate the numerical solutions of the coupled system of bulk-surface reaction-diffusion equations (13) on both the cubic and spherical bulk-surface domains respectively. In all simulations for the coupled system of bulk-surface reaction-diffusion equations (13) we use the values $a_2 = 0.1$ and $b_2 = 0.9$ for parameters in Schnakenberg reaction kinetics. These values are chosen because they lie within a region in parameter spaces corresponding to Turing instability [12,20,34], and therefore satisfies conditions (35)-(40). The other parameters are chosen as $\rho_3 = \frac{2}{5}, \rho_4 = 3, \mu = \frac{2}{5}, \mu_1 = 0, \delta_2 = 0,$ and $\delta_3 = 3,$ so that they all satisfy the parameter compatibility condition (30). We present simulations corresponding to two different cases corresponding to different combinations between diffusion ratios namely d_Ω and d_Γ in the bulk and on the surface respectively. In particular the four combinations of values chosen for the current simulations consist of $(d_\Omega, d_\Gamma) = (30,30), (30,1)$. The theoretical results proposed by Theorem 2.3 are verified numerically by observing that the numerical solution of the coupled system of bulk-surface reaction-diffusion equations (13) induces that if the values of the diffusion ratios are chosen such that $d_\Omega = 30 > 1$ and $d_\Gamma = 30 > 1$, then the finite element numerical solution of the coupled system of bulk-surface reaction-diffusion equations (13) reveals pattern formation in the bulk, on the surface and on the layer of interface where the coupling terms interact through the boundary conditions. It is therefore, when non-linear reaction kinetics are posed both in the bulk and on the surface, with parameter compatibility conditions (30) satisfied and d_Ω, d_Γ much larger than 1, that one may expect the numerical solutions of the coupled system of bulk-surface reaction-diffusion equations (13) to form a spatial pattern everywhere. Figures 9 and 10 show results in agreement with this prediction, which means that spatial pattern can be observed everywhere. Figures 12 and 13 reveal the case where we choose $d_\Omega = 30$ and $d_\Gamma = 1$ for which it was predicted through the results of stability analysis that the reaction kinetics inside the bulk produces spatial pattern with a potential possibility that this pattern may emerge on the surface as well. It is therefore,

if a spatial pattern emerges on the surface under this kind of parameter settings then it does not mean that surface reaction kinetics with $d_\Gamma = 1$ is capable of evolving spatial pattern, in fact it only means that the emerge,nce of spatial pattern on the surface is a consequence of the spatial pattern formed in the bulk and extends through the coupling conditions to appear on the surface.

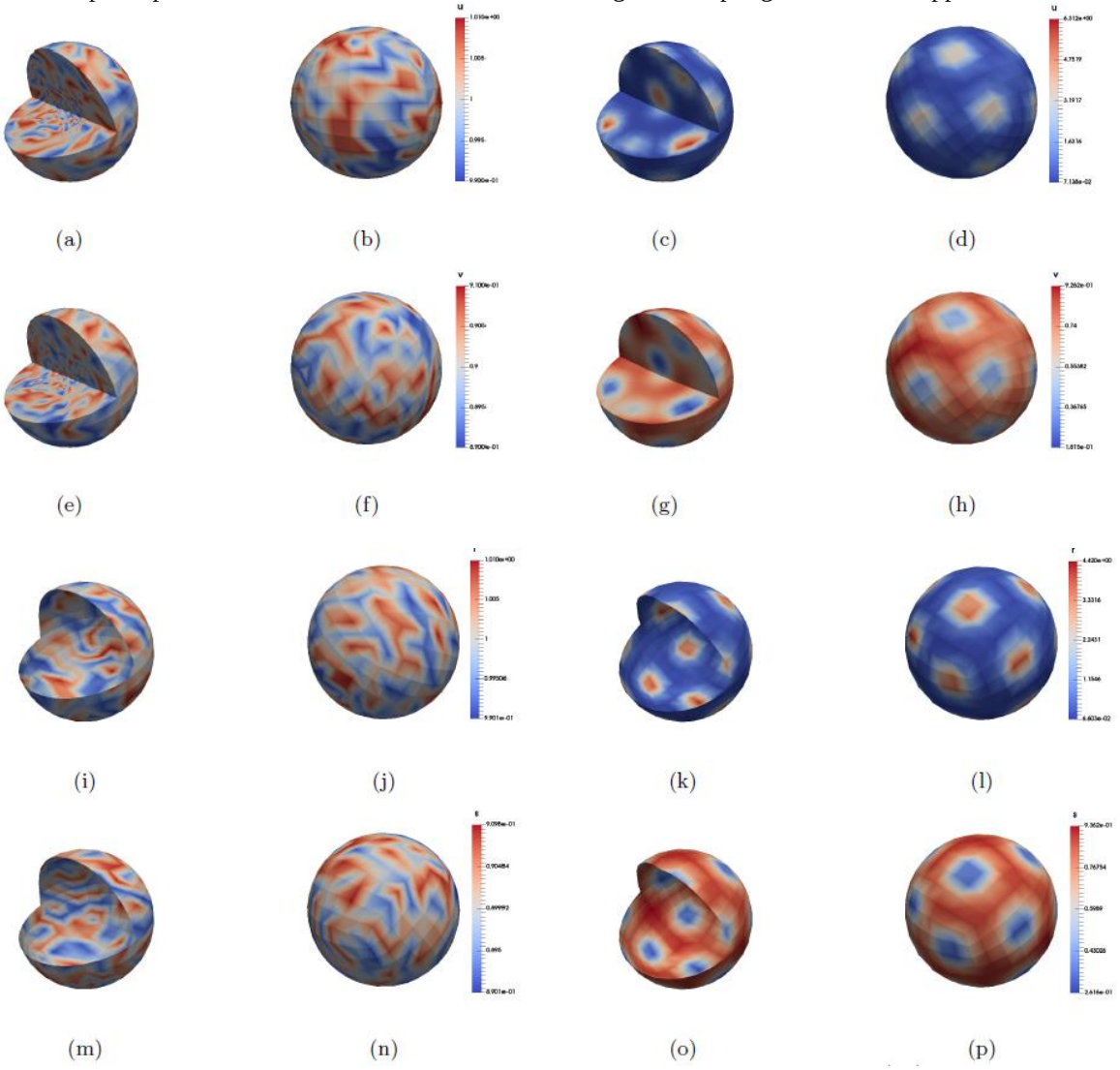

Fig. 9: Numerical solutions corresponding to the coupled system of BSRDEs given by (13) with d_Ω= 30 and d_Γ= 30 and γ_Ω= γ_Γ = 300. The rows correspond to variables u, v, r and s respectively. The first two columns show the initial profile of concentration with random perturbation near the uniform steady state. The third and fourth columns show the bulk-surface finite element numerical solutions at the final time step at time t = 10

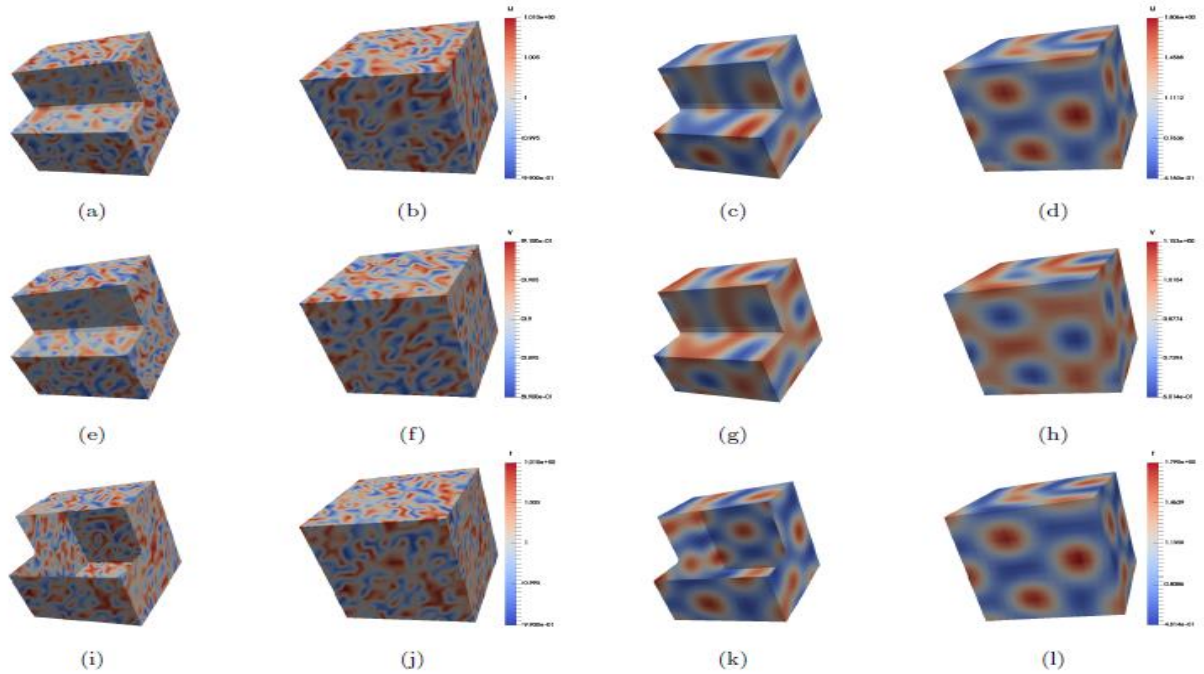

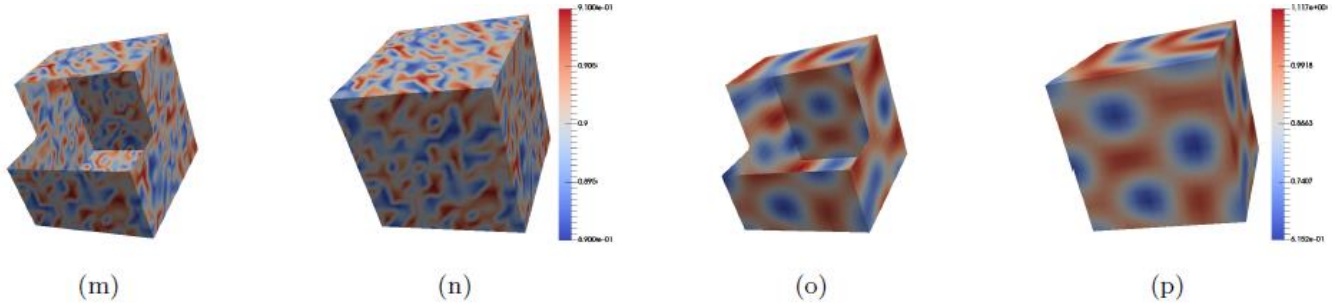

(m) (n) (o) (p)

Fig. 10: Numerical solutions corresponding to the coupled system of BSRDEs given by (13) with $d_\Omega = 30$ and $d_\Gamma = 30$ and $\gamma_\Omega = \gamma_\Gamma = 300$. The rows correspond to variables u, v, r and s respectively. The first two columns show the initial profile of concentration with random perturbation near the uniform steady state. The third and fourth columns show the bulk-surface finite element numerical solutions at the final time step at time t = 10

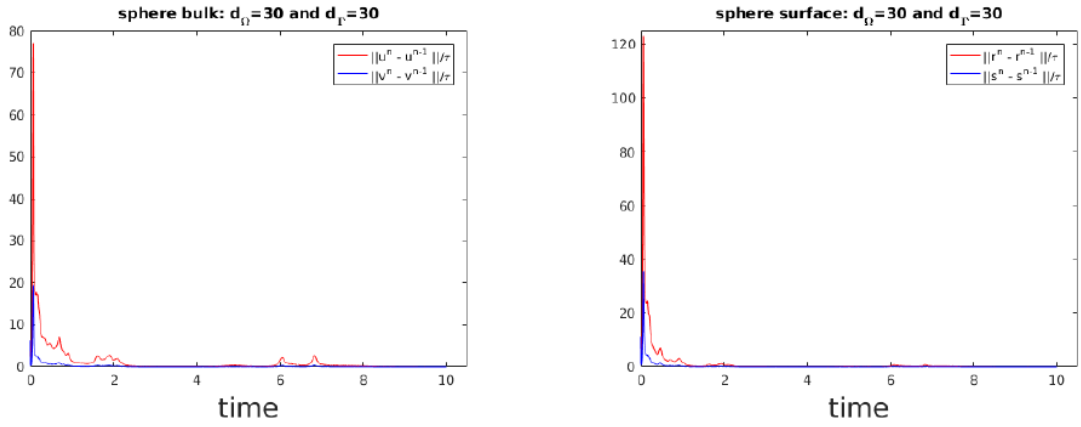

(a) (b)

Fig. 11: Convergence history corresponding to the coupled system of BSRDEs given by (13) with $d_\Omega = 30$, $d_\Gamma = 30$ and $\gamma_\Omega = \gamma_\Gamma = 300$ is shown in the L2 norm of the discrete time derivative. Sub-figure (a) shows the convergence history for the equations in the bulk, whereas Sub-figure (b) shows the same for equations on the surface

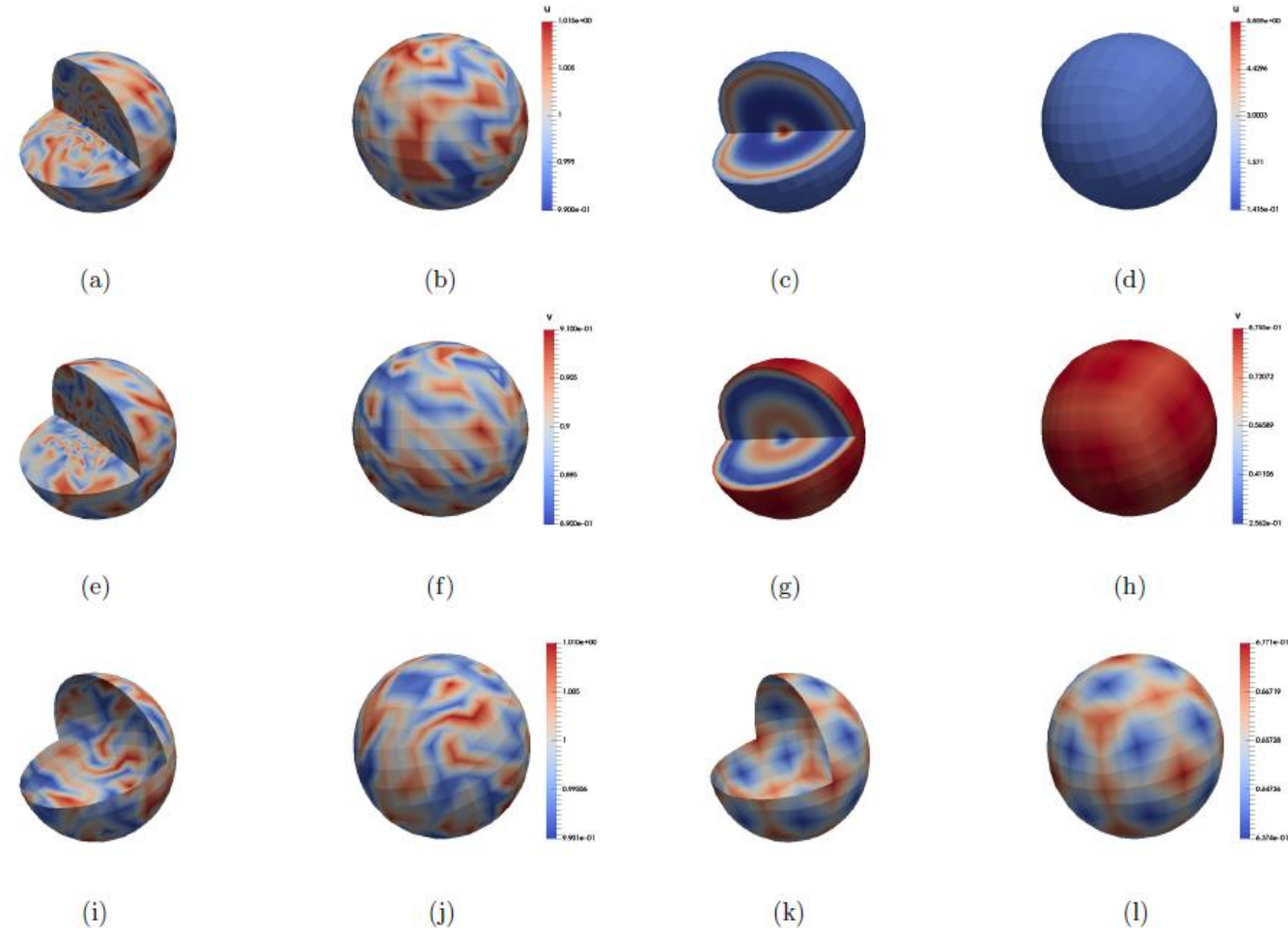

(a) (b) (c) (d)

(e) (f) (g) (h)

(i) (j) (k) (l)

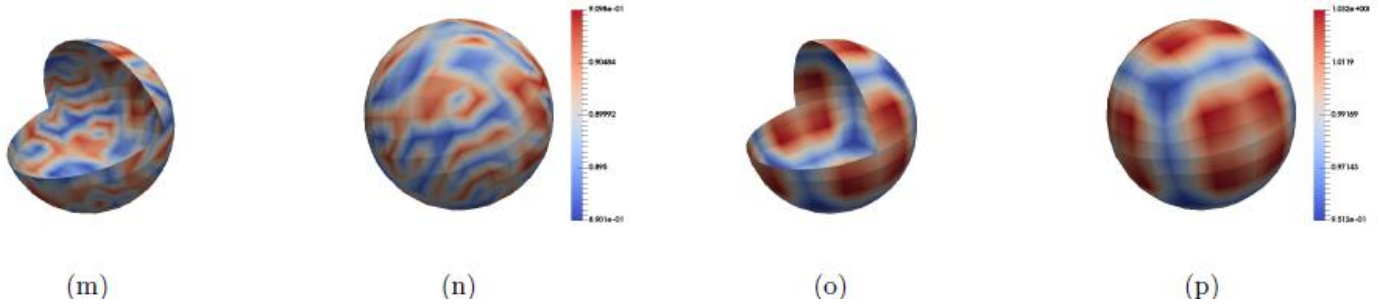

(m) (n) (o) (p)

Fig. 12: Numerical solutions corresponding to the coupled system of BSRDEs given by (13) with $d_\Gamma = 30$ and $d_\Omega = 1$ and $\gamma_\Omega = \gamma_\Gamma = 300$. The rows correspond to variables u, v, r and s respectively. The first two columns show the initial profile of concentration with random perturbation near the uniform steady state. The third and fourth columns show the bulk-surface finite element numerical solutions at the final time step at time t = 10.

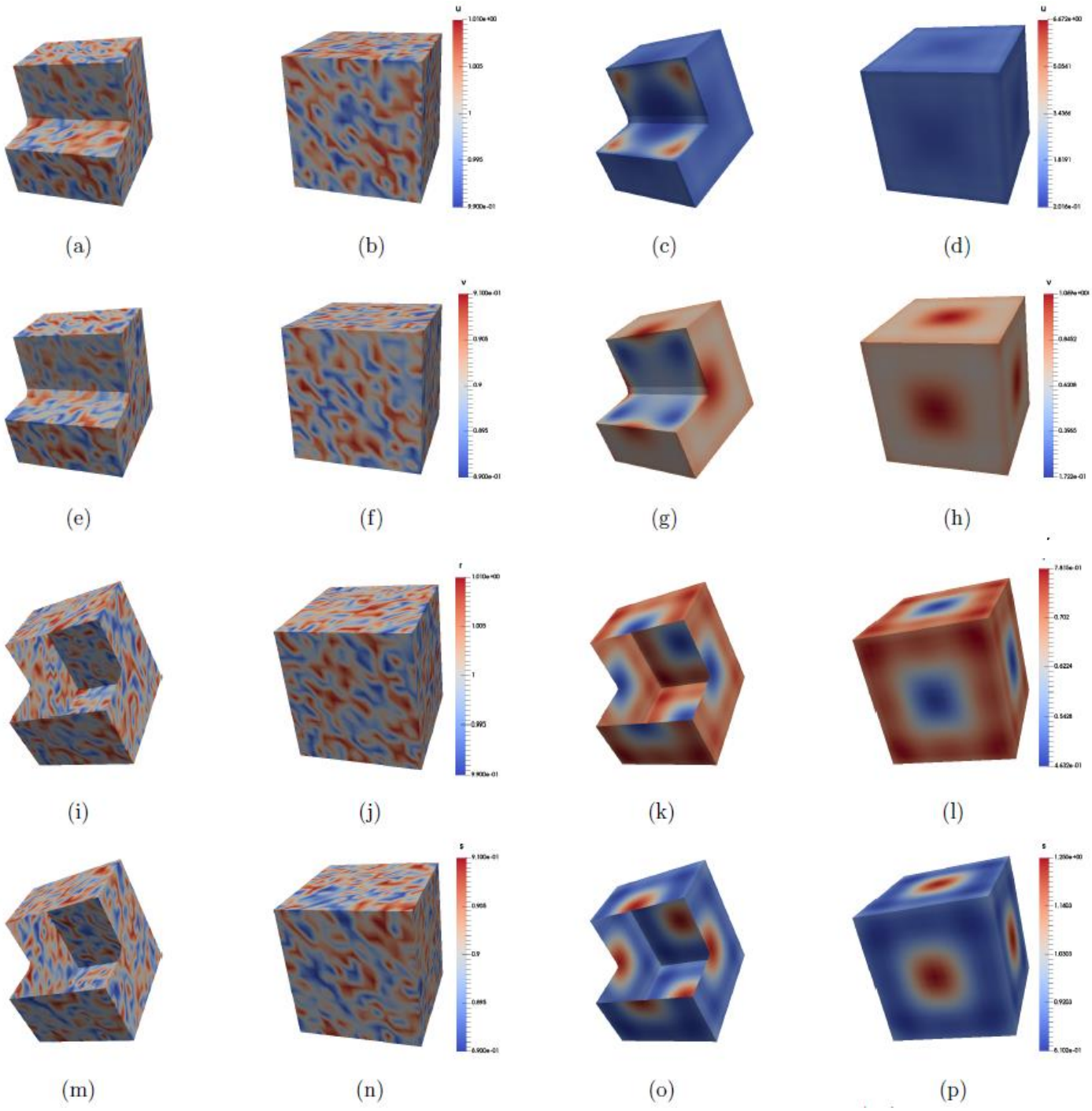

(a) (b) (c) (d)

(e) (f) (g) (h)

(i) (j) (k) (l)

(m) (n) (o) (p)

Fig. 13: Numerical solutions corresponding to the coupled system of BSRDEs given by (13) with $d_\Omega = 30$ and $d_\Gamma = 1$ and $\gamma_\Omega = \gamma_\Gamma = 300$. The rows correspond to variables u, v, r and s respectively. The first two columns show the initial profile of concentration with random perturbation near the uniform steady state. The third and fourth columns show the bulk-surface finite element numerical solutions at the final time step at time t = 10.

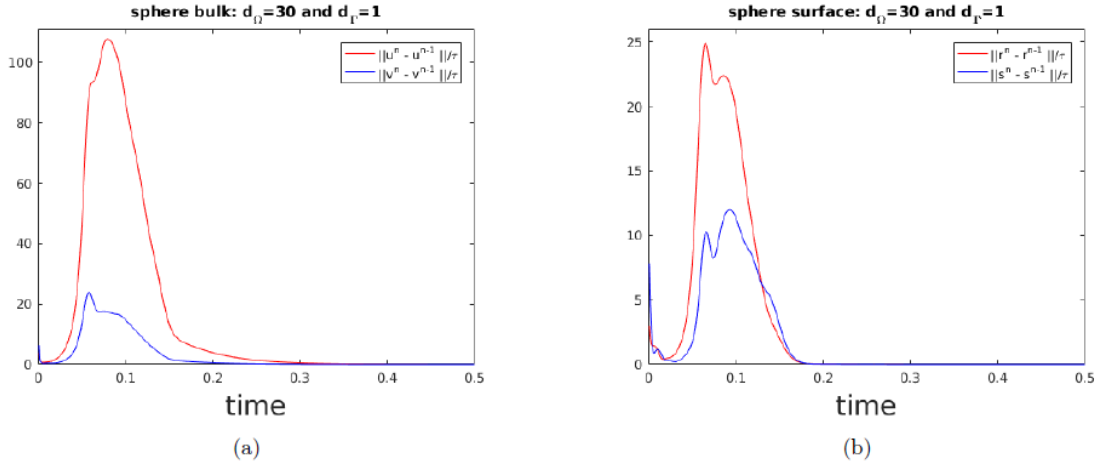

Fig. 14: Convergence history corresponding to the coupled system of BSRDEs given by (13) with $d_\Omega = 30$, $d_\Gamma = 1$ and $\gamma_\Omega = \gamma_\Gamma = 300$ is shown in the L2 norm of the discrete time derivative. Sub-figure (a) shows the convergence history for the equations in the bulk, whereas Sub-figure (b) shows the same for equations on the surface.

6. CONCLUSION

The bulk-surface reaction-diffusion system is explored through studying non-linear reaction kinetics with linear Robin-type boundary conditions. For non-linear reaction kinetics are posed both in the bulk and on the surface, then with appropriate parameter choices, such a system is able to give rise to pattern formation everywhere. Parameters can also be chosen for this system such that pattern emerges in the bulk and extends to the surface, however, it forms no pattern on the internal boundary layer. It is worth noting that the emergence of no pattern in the internal boundary layer is a consequence of parameter choice in the system and not the exhaustive results associated with it. The weak formulation of coupled bulk-surface reaction-diffusion system was obtained to set-up the premises for discretisation in space through employing the standard finite element method. The full coupled system of BSRDEs was simulated using a fully implicit time-stepping scheme through the application of an extended form of Newton's method for vector valued functions. Using fully implicit time-stepping scheme, we numerically demonstrate that this system allows patterns to emerge everywhere. The generality, robustness and applicability of the presented theoretical computational framework for a coupled system of bulk-surface reaction-diffusion equations set premises to study experimentally driven models where coupling of bulk and surface chemical species is prevalent. Examples of such applications include cell motility, pattern formation in developmental biology, material science and cancer biology.

7. REFERENCES

[1] Kondo, S. and Asai, R., A reaction {diffusion wave on the skin of the marine angelfish pomacanthus," Nature 376(6543), 765 (1995).
[2] Janssen, H.-K., On the non-equilibrium phase transition in reaction-diffusion systems with an absorbing stationary state," Zeitschrift fur Physik B Condensed Matter 42(2), 151{154 (1981).
[3] Hutson, V., Reaction-diffusion equations and their applications to biology," Bulletin of the London Mathematical Society 20(2), 185-186 (1988).
[4] Murray, J. D., A pre-pattern formation mechanism for animal coat markings," Journal of Theoretical Biology 88(1), 161-199 (1981).
[5] Mullins, M. C., Hammerschmidt, M., Kane, D. A., Odenthal, J., Brand, M., Van Eeden, F., Furutani-Seiki, M., Granato, M., Ha ter, P., Heisenberg, C.-P., et al., Genes establishing dorsoventral pattern formation in the zebrafish embryo: the ventral specifying genes," Development 123(1), 81-93 (1996).
[6] De Boer, R. J., Segel, L. A., and Perelson, A. S., Pattern formation in one-and two-dimensional shape-space models of the immune system," Journal of theoretical biology 155(3), 295-333 (1992).
[7] Segel, L. A. and Jackson, J. L., Dissipative structure: an explanation and an ecological example," Journal of theoretical biology 37(3), 545{559 (1972).
[8] Keener, J. P. and Sneyd, J., [Mathematical physiology], vol. 1, Springer (1998).
[9] Logan, J. D., [An introduction to nonlinear partial differential equations], vol. 89, John Wiley & Sons (2008).
[10] Turing, A. M., \The chemical basis of morphogenesis," Philosophical Transactions of the Royal Society of London. Series B, Biological Sciences 237(641), 37-72 (1952).
[11] Chechkin, A. V., Zaid, I. M., Lomholt, M. A., Sokolov, I. M., and Metzler, R., \Bulk-mediated diffusion on a planar surface: full solution," Physical Review E 86(4), 041101 (2012).
[12] Murray, J. D., [Mathematical Biology. II Spatial Models and Biomedical Applications Interdisciplinary Applied Mathematics V. 18g], Springer-Verlag New York Incorporated (2001).
[13] Novak, I. L., Gao, F., Choi, Y.-S., Resasco, D., Schaff, J. C., and Slepchenko, B. M., Diffusion on a curved surface coupled to diffusion in the volume: Application to cell biology," Journal of computational physics 226(2), 1271-1290 (2007).
[14] Hansbo, P., Larson, M. G., and Zahedi, S., A cut finite element method for coupled bulk-surface problems on time-dependent domains," Computer Methods in Applied Mechanics and Engineering 307, 96-116 (2016).
[15] Elliott, C. M. and Ranner, T., Finite element analysis for a coupled bulk-surface partial differential equation," IMA Journal of Numerical Analysis 33(2), 377-402 (2013).
[16] Elliott, C. M., Ranner, T., and Venkataraman, C., Coupled bulk-surface free boundary problems arising from a mathematical model of receptor-ligand dynamics," SIAM Journal on Mathematical Analysis 49(1), 360-397 (2017).

[17] Krischer, K. and Mikhailov, A., Bifurcation to traveling spots in reaction-diffusion systems," Physical review letters 73(23), 3165 (1994).
[18] Hagberg, A. and Meron, E., Pattern formation in non-gradient reaction-diffusion systems: the effects of front bifurcations," Nonlinearity 7(3), 805 (1994).
[19] Iron, D., Wei, J., and Winter, M., Stability analysis of turing patterns generated by the schnakenberg model," Journal of mathematical biology 49(4), 358{390 (2004).
[20] Madzvamuse, A., Chung, A. H., and Venkataraman, C., Stability analysis and simulations of coupled bulk-surface reaction-diffusion systems," in [Proc. R. Soc. A], 471(2175), 20140546, The Royal Society (2015).
[21] Wei, J. and Winter, M., Existence and stability of a spike in the central component for a consumer chain model," Journal of Dynamics and Di erential Equations 27(3-4), 1141-1171 (2015).
[22] Yang, W. and Ranby, B., Bulk surface photografting process and its applications.i reactions and kinetics," Journal of Applied Polymer Science 62(3), 533-543 (1996).
[23] Yang, W. and Ranby, B., Bulk surface photografting process and its applications. ii. principal factors affecting surface photografting," Journal of applied polymer science 62(3), 545-555 (1996).
[24] Levine, H. and Rappel, W.-J., Membrane-bound turing patterns," Physical Review E 72(6), 061912 (2005).
[25] Ratz, A. and Roger, M., Symmetry breaking in a bulk-surface reaction-diffusion model for signalling networks," Nonlinearity 27(8), 1805 (2014).
[26] Hahn, A., Held, K., and Tobiska, L., Modelling of surfactant concentration in a coupled bulk surface problem," PAMM 14(1), 525-526 (2014).
[27] Garcke, H., Kampmann, J., Ratz, A., and Roger, M., A coupled surface-cahn-hilliard bulk-diffusion system modeling lipid raft formation in cell membranes," Mathematical Models and Methods in Applied Sciences 26(06), 1149{1189 (2016).
[28] Bruce, A., Johnson, A., Lewis, J., Raff, M., Roberts, K., and Walter, P., Molecular biology of the cell 5th edn (New York: Garland science)," (2007).
[29] Gierer, A. and Meinhardt, H., \A theory of biological pattern formation," Kybernetik 12(1), 30{39 (1972).
[30] Schnakenberg, J., Simple chemical reaction systems with limit cycle behaviour," Journal of theoretical biology 81(3), 389-400 (1979).
[31] Lakkis, O., Madzvamuse, A., and Venkataraman, C., Implicit-explicit time stepping with finite element approximation of reaction-diffusion systems on evolving domains," SIAM Journal on Numerical Analysis 51(4), 2309-2330 (2013).
[32] Prigogine, I. and Lefever, R., Symmetry breaking instabilities in dissipative systems. ii," The Journal of Chemical Physics 48(4), 1695-1700 (1968).
[33] Venkataraman, C., Lakkis, O., and Madzvamuse, A., Global existence for semi-linear reaction-diffusion systems on evolving domains," Journal of mathematical biology 64(1-2), 41-67 (2012).
[34] Madzvamuse, A., A numerical approach to the study of spatial pattern formation. PhD thesis, University of Oxford, UK (2000).
[35] George, U. Z., A numerical approach to studying cell dynamics, PhD thesis, University of Sussex, UK (2012).
[36] Brenner, S. and Scott, R., [The mathematical theory of finite element methods], vol. 15, springer science & business media, Germany (2007).
[37] Bangerth, W., Heister, T., Heltai, L., Kanschat, G., Kronbichler, M., Maier, M., Turcksin, B., et al., The deal. ii library, version 8.3," Archive of Numerical Software 4(100), 1-11 (2016).

